Electrochemical Method for Fabrication of Photovoltaic Fibers based on Tungsten Oxide

By

Linda Magaly Munoz Cordoba

Submitted in Partial Fulfillment of the Requirements

For the Degree of

Master of Science

In the

Chemistry

Program

YOUNGSTOWN STATE UNIVERSITY

August, 2019

Electrochemical Method for Fabrication of Photovoltaic Fibers based on Tungsten Oxide

Linda Magaly Munoz Cordoba

I hereby release this dissertation to the public. I understand that this dissertation will be made available from the OhioLINK ETD Center and the Maag Library Circulation Desk for public access. I also authorize the University or other individuals to make copies of this thesis as needed for scholarly research.

Signature:

_____

Linda Magaly Munoz Cordoba, Student Date

Approvals:

_____

Dr. Clovis A. Linkous, Thesis Advisor Date

_____

Dr. Sherri Lovelace-Cameron, Committee Member Date

_____

Dr. Christopher Arntsen, Committee Member Date

_____

Dr. Salvatore A. Sanders, Dean of Graduate Studies Date

ABSTRACT

Manufacture of photovoltaic (PV) clothing, which can absorb sunlight and generate an electrical potential, has long been an objective for the military and for avant-garde fashion designers. Early designs simply consisted of pinning small PV modules onto regular garments. A more sophisticated approach has emerged, where the objective is to deposit PV material on the individual threads of the textile. That is the primary focus of this research: to develop a procedure for fabricating a photovoltaic cell, using tungsten oxide, WO_3, as the semiconductor PV material and steel thread as the substrate. Various procedures for making thin films of WO_3 via electrodeposition were examined. All of the procedures started by preparing a plating solution of peroxotungstate ion, $W_2O_{11}^{2-}$. It was found that Pt black powder should be added to the solution after $W_2O_{11}^{2-}$ formation to consume excess hydrogen peroxide. Purging the solution with Ar before electrodeposition and stirring it during electrodeposition increased the deposition rate. Annealing the WO_3 film at 450 ^oC was necessary to form a stable oxide, but it also caused shrinkage, resulting in a segmented coating on the steel thread. This coating was electroactive but not photoactive. The effect of substrate was examined by depositing WO_3 on In-doped tin oxide (ITO). The WO_3 film on ITO was uniform, but quite fragile, and did not exhibit any photoeffects. Thus while electroactive WO_3 films could be fabricated, the desired photoeffect was not observed. Future work should concentrate on the junction characteristics of these films, which must exhibit solid state depletion layer behavior to be an effective PV device.

ACKNOWLEDGEMENTS

I would like to thank my advisor Dr. Linkous, for all his support and accompaniment in this project. I would like to thank to Dr. Sherri Lovelace – Cameron and Dr. Christopher Arnstsen, who are part of the thesis committee. I would like to thank Ray Hoff for all his help with the instrumentation and my research group for all their unconditional support. Finally, I want to thank my family because they all sacrificed themselves, so that I could advance with my education.

TABLE **OF CONTENTS**

TABLE OF FIGURES

LIST OF TABLES

Chapter 1.

INTRODUCTION

Worldwide energy consumption is growing quickly, causing two problems. The first one is global Warming and the other one is “Hubbert’s Peak” theory, which says that reducing the rate of discovery of the fossil fuels will ultimately cause a decrease in oil production , despite the fact that energy demand will have increased. U.S. statistics show solar energy has been growing slowly in the last 8 years, but it nevertheless predicts significant growth for it (1). Solar energy growth could be possible through research in electric power production and water splitting for hydrogen generation using this free energy. The primary focus of this research will be electric power production by photovoltaic clothing. Electric power production via photovoltaic clothing will help to reduce greenhouse gases and pollutants from fossil fuels. Other advantages are: its use in remote locations, which reduces the loss of electricity due to distribution, reduces water consumption the electric generation process, is free, provides energy independence, etc. The use of solar energy requires a semiconductor material that converts sunlight to electricity. The use of metal oxides for trapping solar energy is a potential technology. Tungsten oxide is a semiconductor metal oxide with band gap energy (2.8 eV) larger than the common silicon semiconductors (1.1 eV); this fact has generated interest for this material. Photovoltaic clothing using tungsten oxide could be a good match due to it being a material which collects electricity easily because of its large bandwidth and it being very stable. This thesis research intends to create a photovoltaic cell using

tungsten oxide as a semiconductor material and a commercial conducting steel thread like substrate for the purpose of producing electricity for charging a device.

1.1 Background:

Nowadays, according to U.S Energy Information Administration, around 64% of electric power comes from fossil fuels, mainly from coal and natural gas. Renewable energy sources only cover 13%.

Electric power production and water splitting for hydrogen generation are some of the technologies that are being developed to use solar energy (2) .

Energy from hydrogen appears very promising because it is an abundant element; it has the highest heat of combustion per unit weight of any chemical compound (120,000 kJ/kg), and it can be electrochemically oxidized. Although hydrogen has many advantages, it has some problems as well. One of the problems is that hydrogen mostly exists in combined form in Nature so that energy must be expended to recover the H_2 as the diatomic gas. However, this recovery energy may just be a fraction of the ultimate heating value (3).

Electric power production from the sun is another important technology that helps to decrease the consumption of fossil fuels, which leads to less production of greenhouse gases and other pollutants. In addition, it is good for remote applications, reducing the loss of electricity due to distribution. It also reduces water consumption in electric generation processes and promotes sustainability and energy independence, etc.

The most direct method for converting solar energy for both hydrogen production and electric power is photovoltaics (PV). It requires a semiconductor material to convert the sunlight. The use of certain metal oxides for trapping the solar energy is a potential technology (2).

Tungsten oxide is a semiconductor metal oxide with a band gap energy that is larger than the common silicon (1.1 eV) semiconductors (4). "TiO_2 is relatively high (3.2 eV) and, hence, it is only capable of absorbing 5-7% of the solar spectrum. Unlike TiO_2, WO_3 has considerably smaller band gap energy (2.6 eV) and is, therefore, capable of increased absorption in the visible light region (about 12% of the solar spectrum)" (5). This characteristic has generated interest for this material.

Functional clothing is a discipline that integrates the conventional clothing concept with other areas, such as medicine, biotechnology, nanotechnology, etc. Nowadays, there are many functional clothing products available in the market. The products have different applications, e.g. Protective military armor, protective surgical gowns for the doctors, and photovoltaic clothing, etc. Photovoltaic clothing presently consists of macroscopic photovoltaic cells attached to regular woven fabric. It could generate electricity far from any main supply and it could power electronic devices. In this technology, the photovoltaic cell (PVC) is deposited onto a fiber and the energy that it produces is more than the required for portable devices.

Photovoltaic clothing using tungsten oxide could be a good match due to its stability in air and water, particularly acidic solutions, and because it is a very stable material, with a high melting point (1473°C), enabling it to hold up under most

processing conditions. In addition, this material resists-photo-corrosion under illumination and can absorb visible light (6).

A thread substrate is very important for clothing since it gives flexibility. It means more comfortable clothing for people; however, it has other associated problems related to the movement of the fibers, that cause interconnects troubles.

Despite the mentioned problems, this research intends to create a PV cell using tungsten oxide as a semiconductor material and a commercial conducting steel thread as substrate.

Other tungsten oxide applications are the following: pigment in ceramics and paints, photo electrochemical water splitting, gas sensors, and smart windows, which are electrically switchable glass that change light transmission properties with an applied voltage (7).

1.2 Photovoltaic Effect:

The photovoltaic effect is the creation of voltage in a material upon exposure to light". (8)

1.3 Electrodeposition:

It is deposition process in which ions are oxidized or reduced to a neutral state and deposited on the surface of an electrode by the passage of electric current. Electrodeposition is a very accepted technique for electrode preparation due to its simplicity and low cost.

Electrodeposition Technique:

Electrodeposition means coating a thin layer of a metal to modify its surface properties. For example, nickel or chromium metal is electrodeposited on automotive products for avoiding corrosion. According to Nanostructured Tungsten Oxide – Properties, Synthesis, and Applications, the following steps happen in electrodeposition: " i) The formation of isolated nuclei and their growth to larger grains, ii) The aggregation of grains, and iii) The formation of crystallites' (7).

Electrodeposition advantages:

The tungsten oxide layer will be prepared by electrodeposition. This technique has many advantages to be cited, for example:

- It produces growth of any shape and size. This property is very relevant due to the electrodeposition could be on a thread instead of a steel substrate.
- It is commonly and easily performed at room temperature.
- The film properties could be changed just as the bath composition and the applied voltage varies.
- It is an inexpensive procedure.
- It is amenable to metal deposition, since the freshly deposited layer become conductive and can serve as an active surface for subsequent layers.

1.4 Tungsten oxide:

Blue oxide:

These are obtained by mild reduction of acidified solutions of tungstate or of suspensions of WO_3 in water. The blue state can also be generated electrochemically when a thin WO_3 film on a conductive substrate is subjected to a negative polarization. This is the basis of WO_3's use in electrochromic devices. A detailed electronic explanation for the blue color has not been found (9).

1.5 Semiconductor:

Semiconductors are crystalline materials with conductivities between that of a conductor and an insulator. Some semiconductor materials are elemental silicon and germanium, doped oxides such as titanium dioxide, ferric oxide, and tungsten oxide, intermetallic compounds, such as silicon carbide and gallium arsenide, and variety of organic compounds (8).

1.5.1 Doping:

Doping helps to enhance the conductivity of a wide band gap crystal. A tiny, controlled amount of impurity is introduced into the crystal. There is a replacement between the atoms in the lattice of the crystal and atoms from the impurity, so if an impurity with higher valence is inserted, there will be one or more unbound electrons in the structure; only a small amount of thermal energy is then needed to free this electron for conduction. For example, silicon crystal could be doped with group V elements, such as arsenic (8).

1.5.2 Holes:

The hole occurs when thermal excitation of an electron leaves a positively charged region, named a "hole." The hole helps with the electrical conductance of a crystal. The hole movement is stepwise, in that a bound electron from a neighboring atoms jumps to the electron – deficient region and leaves a positive hole in its wake (8).

1.5.3 Tungsten Oxide as n–type semiconductor:

N-type refers to a semiconductor that has been doped, so that it contains nonbonding electrons. N-type or negative type is associated with the fact that negatively charged electrons are the majority carriers of charge (8). N-type doping in WO_3 is achieved by vacancy doping, i.e., making the crystal slightly substoichiometric with respect to oxygen.

1.6 Pourbaix diagram of WO_3 :

Pourbaix diagram is a potential – pH diagram. It was prepared by Marcel Pourbaix (1963), an electrochemist and corrosion scientist. It shows the metal stability as a function of the potential and pH. The diagram is useful for the following: (i) it gives reactions directions, (ii) it can predict corrosion (10). Figure 1 shows ´´Tungstate surface oxides in acid media. In alkaline media, soluble tungstate ions are formed´´. Pourbaix diagrams address aqueous chemistry only (11), (12).

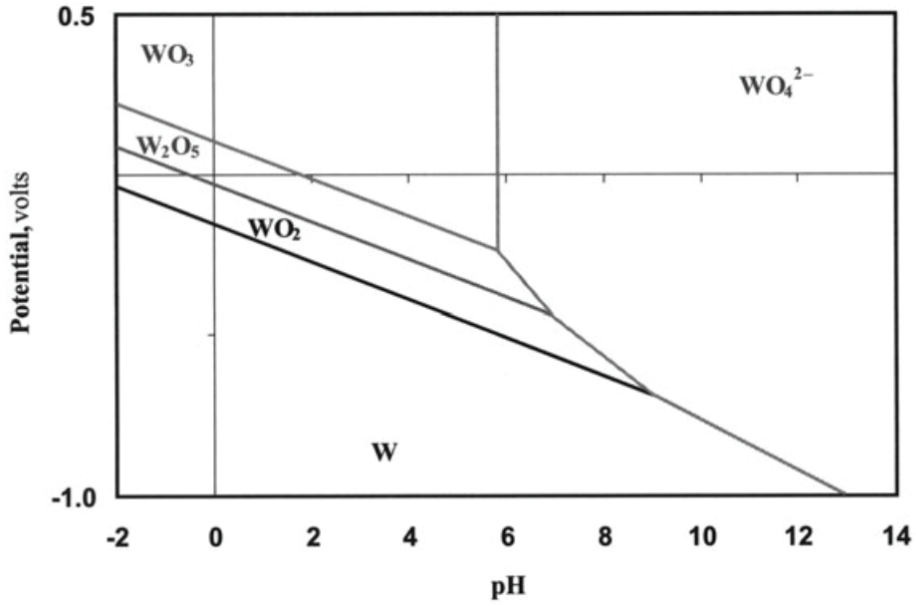

Figure 1. Pourbaix diagram for tungsten in water (11)

1.7 Research Problem and Approaches

1.7.1 Purpose Statement:

The main goal of this research is tungsten oxide electrodeposition on a steel thread for photovoltaic clothing application.

Previous research used flat strips of stainless steel 304 as a substrate for WO_3 films, but this research will focus on steel thread. However, the steel-strip will be evaluated as well, in order to compare its morphology and photovoltaic properties vs. the steel thread.

1.7.2 Importance of this research:

Photovoltaic clothing, which traps the sunlight and then produces electricity, is a technology that takes advantage of the free solar energy. This energy could be useful for electronic charging devices. It will help people in rural areas where there are power supply problems, and without the environmental pollution derived from fossil fuels. It could be useful for soldiers in the field for recharging their batteries without carrying heavy equipment.

Chapter 2.- Materials and experimental procedures:

2.1 **Reagents and materials:**

Platinum black powder (Johnson Matthey)

Sodium tungstate dihydrate (Sigma-Aldrich)

Hydrogen peroxide 30% (Fisher Chemical)

Chloroplatinic acid (Sigma-Aldrich)

Perchloric acid

Stainless Steel Thread (13)**:**

It was bought from adafruit.com. It is thin, strong and smooth. ´´This thread is 2 ply, a little thicker than every day polyester or cotton thread but still thin enough to be sewn by hand in medium-eye needles or with a sewing machine that can handle 'heavy' thread. Because it is strong and smooth, it's ideal for any wearable/e-textile project. It also has fairly low resistivity, 16 ohms per foot so you can use it to drive LEDs and other electronic components that use under ~50mA. Because it is made of stainless steel fibers, it will not oxidize like silver does´´ (13).

The setup for the electrodeposition experiment requires the following three electrodes; working electrode, reference electrode and counter electrode. The electrodes are connected to the potentiostat, which controls the currents into the solution. The electrodes are into a vessel that contains the ionic solution where the reactions are going on.

Figure 2 shows the setup.

Figure 2. Three-neck round bottom flask with the electrolyte solution for electrocepositing tungsten oxide

2.2 Approach I: sodium tungstate dissolved in 30% hydrogen peroxide

The following 25 mM solution was prepared: The solute was sodium tungstate and the solvent was 30% hydrogen peroxide. After 10 days under stirring and 25°C, the pH eventually rose to around 7.6. The peroxotungstate formation is best described as:

$$2WO_4^{-2} + 4H_2O_2 \rightarrow W_2O_{11}^{-2} + 2OH^- + 3H_2O$$

The important point is that 2 moles of tungstate ion make 2 moles of hydroxide, or equimolar amounts. After 10 days, the OH^- concentration does not match the initial

concentration of tungstate because it was used up in acid/base chemistry with the peroxide.

Once a 7.6 pH is reached, the second step is to add concentrated perchloric acid dropwise to reduce pH to 1.2. The solution is then ready for the electrodeposition.

The experiment tested the steel thread (working electrode) with and without a cleaning procedure before the electrodeposition. The cleaning procedure was the following: clean with detergent, then clean with acetone, methanol, deionized water and finally air dried.

The temperature of the electrodeposition experiment was 25 °C; the applied voltage was -0.50 V vs. silver chloride (reference electrode). The experiment ran for 45 minutes.

Electrodeposition testing was done using a PAR 273A potentiostat, in a conventional single compartment cell, with a three-electrode setup, consisting a rolling steel thread electrode (working electrode), silver chloride electrode (0.22 V – reference electrode) and a platinum foil (100 mm^2 surface area – counter electrode). Working electrode potential was measured relative to the reference electrode, which has a known and stable electrode potential.

The reaction of interest is the following:

$$2W_2O_{11}^{2-}(aq) + 8H^+(aq) + 4e^- \rightarrow 4WO_{3(s)} + 4H_2O + 3O_{2(g)}$$

2.3 Approach II: Reduced H_2O_2/Na_2WO_4 proportion

Approach II tried to improve on approach I, in that it does not use as much peroxide in the peroxyditungstate formation; instead, it used a solution with a volumetric ratio of 80% of 30% H_2O_2 and 20% of 25 mM Na_2WO_4. In addition, it used platinum black powder, in a concentration of 0.03 mg/ml. The solution was stirred vigorously for 1 hour and 20 minutes until it reached a pH about 10.5.

Figure 3 shows the peroxotungstate formation in the initial time (a) and when it reaches 10.5 pH (b). The right beaker contains the Approach I solution and the left beaker contains the Approach II. The right beaker looks exactly the same in pictures a and b (approach I). However, the left beaker (Approach II) changes, if the pictures a and b are compared. The color turns from a turbid pale yellow to transparent, and the pH changes as well from 7 to 10.5.

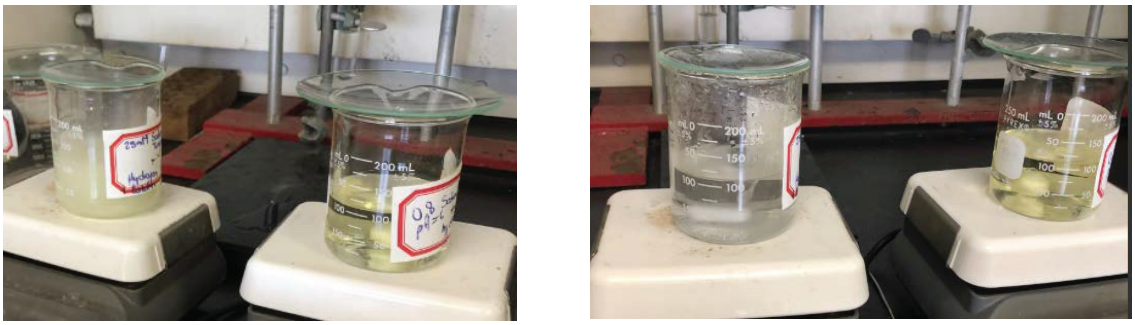

a b

Figure 3. Peroxotungstate formation. Right beaker in both pictures contains Approach I and left beaker contains Approach II. a. Initial time, b. reaction after 1 hour.

Once the solution reaches 10.5 pH, it is filtered by a vacuum to remove the Pt black powder, and then the solution is acidified with perchloric acid to a pH of 1.20. Then the solution is ready for the electrodeposition.

Approach II subjected the steel thread (working electrode) to a cleaning procedure before the electrodeposition. The cleaning procedure was the same as previous: clean with detergent, then acetone, methanol, deionized water and finally air dried.

The temperature of the electrodeposition experiment was 25 °C; the applied voltage was -0.50 vs. silver chloride (standard electrode) and lasted 1.5 hours. Electrodeposition testing was done using a PAR 273A potentiostat, in a conventional single compartment cell, with a three-electrode setup, consisting a rolling steel thread electrode (working electrode), silver chloride electrode (0.22 V – reference electrode) and a graphite electrode (counter electrode).

Once the electrodeposition was done, to increase the grain size of the tungsten oxide, the strip was heated until it reached 450 °C during 1 hour (7).

2.4 Approach III: Stirring, purging and annealing under argon

In Approach III, the solution was prepared in the same way as approach II. The main difference is in the electrodeposition, in that the solution was purged with argon gas for at least 10 minutes before the experiment and the electrolyte was stirred during electrodeposition. Another difference is that annealing was performed under argon flow.

Approach III tested the steel thread and the stainless steel strip with the same cleaning procedure used in approach II.

The temperature of the electrodeposition experiment was 25 °C; the applied voltage was -0.50 V vs. silver chloride (standard electrode) and it lasted 1.5 hours. Electrodeposition testing was done using a PAR 273A potentiostat, in a conventional

single compartment cell, with a three-electrode setup, consisting of a rolling steel thread or stainless steel strip electrode (working electrode), silver chloride electrode (0.22v – reference electrode) and a graphite electrode (counter electrode).

Once the electrodeposition was done to increase the grain size of the tungsten oxide, the strip was heated. Two temperatures were tested, 450 °C and 600 °C, with argon flow.

2.5 Approach IV: Platinum addition

In approach IV, the solution was prepared in the same way as approach III. The difference is at the end of the electrodeposition process; three minutes before it finished, 1 mM of chloroplatinic acid hexahydrate is poured to the electrolyte. The idea was to deposit a few atomic layers of Pt. The one millimolar concentration served to give you a reasonably effective thickness. It is around 0.2 µm. It was calculated with the Equation 1. Film Thickness:

$$\text{Thickness (m)} = \frac{\text{Current} * \text{Electrolysis time x Atomic weigth Pt}}{\text{Stoichiometric Pt number x Faraday´s constant x Electrode area x Density of solid Pt}}$$

Equation 1. Film Thickness

The variables were the following:

Current = 1.6 x 10^{-4} C/s, it comes from Figure 76

Electrolysis time = 180 s

Atomic Weight Pt = 195 g/mol

Stoichiometric Pt number = 4 equiv/mol

Faraday´s constant = 96485 C/equiv

Electrode area = 0.1 m^2

Density of the solid Pt = 21.45 g/cm^3

Approach IV tested the steel thread with the same cleaning procedure used in Approach I.

The temperature of the electrodeposition experiment was 25 °C; the applied voltage was -0.50V vs. silver chloride (standard electrode) and it lasted 1.5 hours. Electrodeposition testing was done using a PAR 273A potentiostat, in a conventional single compartment cell, with a three-electrode setup, consisting of a rolling steel thread electrode (working electrode), silver chloride electrode (0.22 V – reference electrode) and a graphite electrode (counter electrode).

Once the electrodeposition was done to increase the grain size of the tungsten oxide, the strip was heated until it reached 450 °C under argon flow.

2.6 Approach V: The same approach III solution with ITO as a substrate

In approach V, the solution was prepared in the same way as approach III. The difference is that instead of conductive thread, indium-doped tin oxide (ITO) is the substrate.

Approach V tested the ITO with the same cleaning procedure used in approach I. The temperature of the electrodeposition experiment was 25 °C; the applied voltage was -0.50 V vs. silver chloride (reference electrode) and it lasted 1.5 hours. Electrodeposition testing was done using a PAR 273A potentiostat, in a conventional single compartment cell, with a three-electrode setup, consisting of ITO piece (working electrode), silver chloride electrode (0.22 V – reference electrode) and a graphite electrode (counter electrode).

Once the electrodeposition was done to increase the grain size of the tungsten oxide, the ITO piece was heated until reached 450 °C in air.

Chapter 3 - Techniques used for characterization

3.1 Thermogravimetric analysis (TGA)

Thermogravimetry helps to analyze decomposition reactions and its chemistry involved. The instrument uses nitrogen or argon to create an inert atmosphere throughout the test. The TGA has three parts: a high temperature furnace, a sample holder and a balance. It gives a thermogram as a final result. The thermogram shows the change in weight (gain or loss) as a function of temperature. Before running the experiment, a sample of test material is placed in an aluminum cup that is suspended from an analytic balance located outside the chamber. The balance sends a weight signal to the computer, and it plot the thermogram. The Y-axis on the thermogram plot shows weight (grams or milligrams) and the X-axis has the reference material temperature (2). The analysis of the plot allows one to determine the temperature range at which the sample begins to decompose. Figure 4 shows the TGA that was used in this research (TGA 2850 Thermogravimetric Analyzer – TA Instruments).

Figure 4. Thermogramimetric analyzer

3.2 Scanning Electron Microscopy (SEM)

Scanning electron microscopy is a powerful analytical technique for evaluating the morphology of solids, becauseto it is capable of imaging at high magnification. This instrument has a beam of electrons, which are emitted thermionically from a cathode and accelerated toward an anode. The cathode could be made from tungsten or lanthanum hexaboride for their high melting point and low vapor pressure; at YSU the filament in the SEM is a single crystal of lanthanum hexaboride. The beam is focused by one or two condenser lenses into a beam with a very fine focal point. The beam passes through pairs of scanning coils or pairs of deflector pairs in an optical column which deflects the beam horizontally and vertically so that it scans in a raster fashion over a rectangular area of the sample surface. The energy exchange between the electron beam and the sample can be detected to produce an image (2).

The instrument used in this research is a JEOL JIB-4500 multi beam system, as shown in Figure 5.

Figure 5. Scanning electron microscopy

3.3 X-ray Diffraction

X-ray diffraction is a technique used for the study of crystal structures and atomic spacing. It is based on the constructive interference of X-rays that are generated by an X-ray tube. In the experiment, the X-rays are produced by a copper anode and filtered to produce monochromatic radiation. Then the X-rays are collimated to straighten the beam, and directed toward the sample. In these kinds of experiments, the samples have polycrystalline structures. In theory, there are thousands of grains that have random orientations in the film. Scanning through an angle θ of incident x-ray beam from 0° to 90°, it is possible to find all the angles where diffraction occurred. Every one of these angles are associated with a different atomic spacing. The X-ray interaction produces a

constructive interference and satisfies Bragg's law. The technique uses the Bragg equation to convert 2θ for each diffraction peak to d-spacing.

$$n\lambda = 2dsin\theta$$

The unit has a goniometer and a detector which records the x-ray coming out of the sample and it sends the information to the computer. The idea is to compare d-spacing with reference patterns. There are data bases with many crystal spectra, so it is necessary to match the spectrum that was obtained with the database. Comparing the unknown diffraction pattern with the database makes the identification easier (2), (14). The instrument used for characterizing the WO_3 deposits is shown in Figure 6.

Figure 6. X-ray diffraction apparatus- YSU laboratories

3.4 Electrochemistry measurements

Cyclic voltammetry (CV) is an electrochemical technique which measures the current that develops in an electrochemical cell under conditions where voltage is swept

through an electro-potential range. This electro analytical technique allow us to study electroactive anodes rapidly. It evaluates the redox behavior easily over a wide potential range. The technique requires a waveform generator to produce the excitation signal, a potentiostat to apply this signal to an electrochemical cell, a current-to-voltage converter to measure the resulting current and a computer to display the final results. It produces a voltammogram as a result, which displays current on the Y-axis versus potential on the X-axis. Due to the potential being proportional with time; the X-axis can be time axis as well. A Princeton Applied Research (PAR) potentiostat/galvanostat model 273A was used for this research, and is shown in Figure 7. The cell has a conventional single compartment, with a three-electrode setup, consisting of steel thread electrode (working electrode), silver chloride electrode (reference electrode) and a platinum foil or graphite (counter electrode). The light source used is Newport solar simulator, which has a xenon lamp (Newport 500W and 1000W were used in this research) (2).

Figure 7. Potentiostat/galvanostat model 273A

3.4.1 Cyclic Voltammetry Standards:

Before focusing on the tungsten oxide electrodeposition, other standard deposition behaviors were studied in order to have them as patterns to compare with tungsten oxide deposition. The system that was studied was 0.01 M $CuSO_4$ in 0.1 M H_2SO_4, pH=1. The standards were the following:

- **First standard:** this is a very common electrodeposition behavior

Working Electrode (WE): Stainless Steel

Reference Electrode (RE): Silver Chloride

Counter Electrode (CE): Platinum

A picture of the stainless steel electrode after copper deposition is shown in Figure 8 , and its electrochemical behavior is shown in Figure 9.

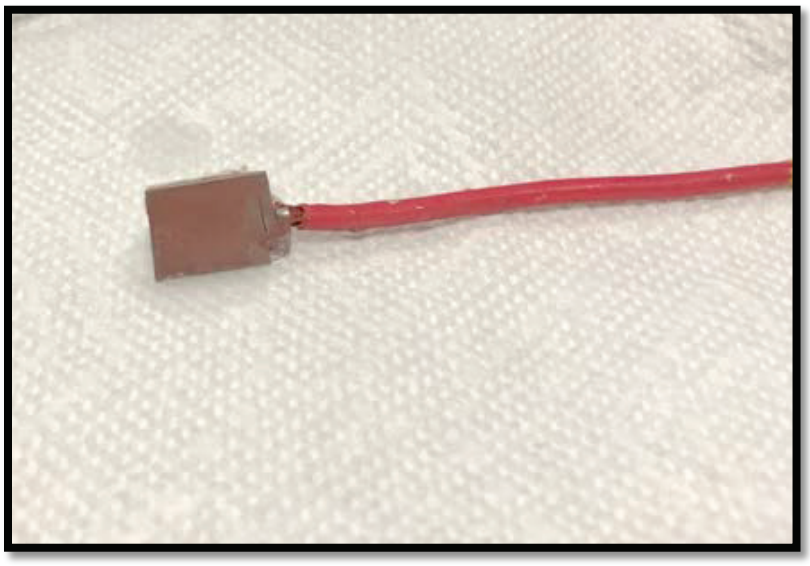

Figure 8. Cu deposition on steel electrode once cyclic voltammetry test was done

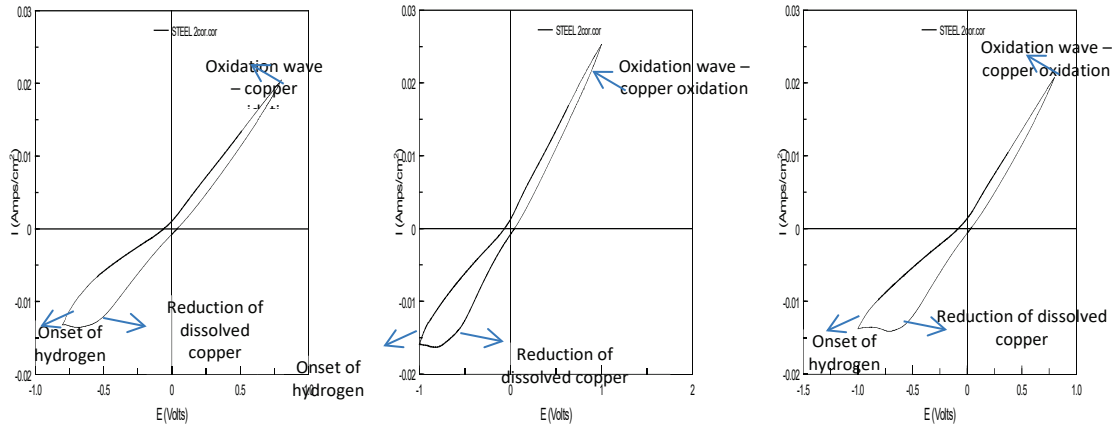

a b c

Figure 9. Cyclic voltammetry curves for stainless steel 304 electrode in 0.01M $CuSO_4$ - 0.1 M H_2SO_4; voltage ranges: a. (-0.8 – 0.8) V; b. (-1 - 1) V; c. (-1 – 0.8) V vs Ag/AgCl

All the cyclic voltammetry curves have a very similar shape, even though they have different voltage ranges. They show a linear increase in the oxidation wave, due to copper oxidation. The lower peak on the right shows reduction of the dissolved copper ion to the metallic state on the electrode, and the other lower peak on the left is the onset of the hydrogen evolution.

- **Second standard:** this system has an unusual behavior because the oxidation occurs in excess.

Working Electrode (WE): Copper

Reference Electrode (RE): Silver Chloride

Counter Electrode (CE): Platinum

The Cu working electrode and its voltammetry behavior are shown in Figure 10 and Figure 11 respectively.

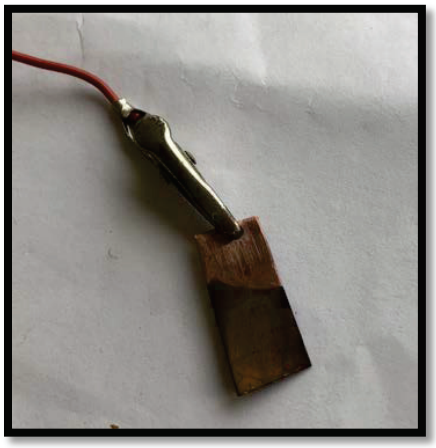

Figure 10. Copper electrode after the cyclic voltammetry test was done.

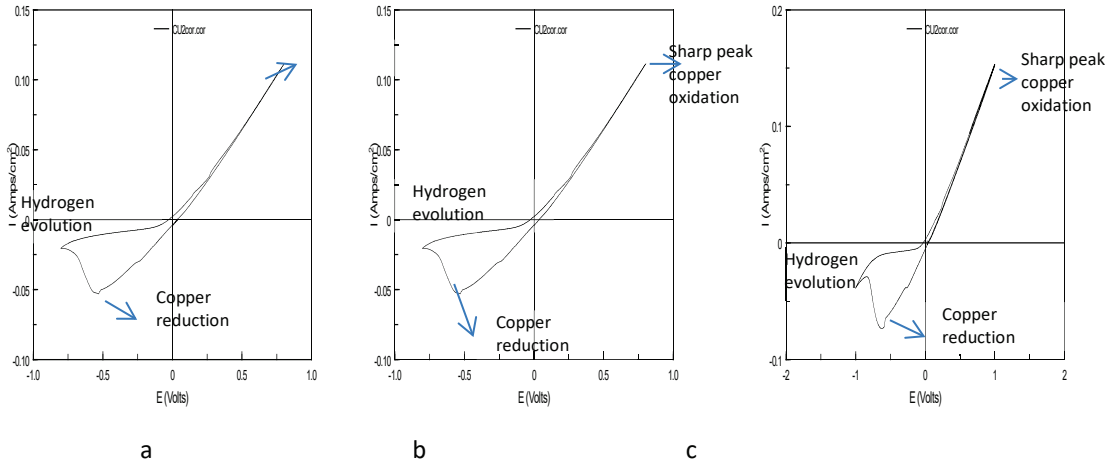

Figure 11. Cyclic voltammetry curves for Cu electrode in 0.01M $CuSO_4$ - 0.1 M H_2SO_4; voltage ranges: a. (-0.8 - 0.8) V; b. (-0.7 - 0.7) V; c.(-1 - 1) V.

All the cyclic voltammetry curves look very close, especially the curves a and b which are almost the same. The curves show an unusual copper oxidation behavior with the sharp peak on the upper right, and they show two reduction peaks on the left. The lower peak on the left shows hydrogen evolution for the sulfuric acid present and the other lower peak shows the copper reduction.

- **Third standard:** this system has ideal behavior.

Working Electrode (WE): Graphite rod

Reference Electrode (RE): Silver Chloride

Counter Electrode (CE): Platinum

The working electrode and its voltammetric behavior are shown in Figure 12 and Figure 13, respectively.

Figure 12. Inert graphite electrode

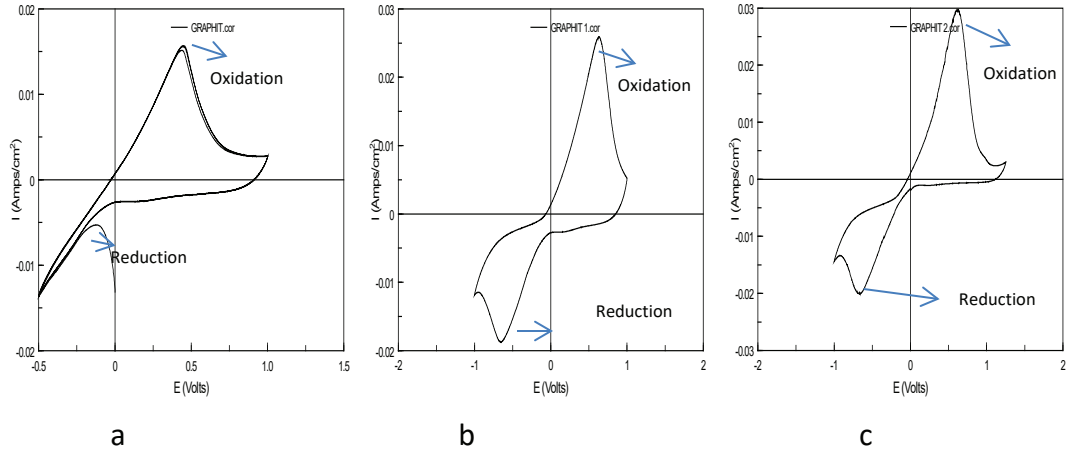

Figure 13. Cyclic voltammetry curves for graphite electrode in 0.01M $CuSO_4$ - 0.1 M H_2SO_4; voltage ranges: a. (-0.5 – 1.0) V; b. (-1 – 1.0) V; c. (-1 – 1.25) V.

Both oxidative and reductive desorption behavior was observed. The deposited copper is completely oxidized off the surface of the graphite electrode. Hence the current reaches a peak value and then decays to the baseline.

3.4.2 Cyclic Voltammetry (Perchloric Acid, pH = 1.0) – Blank of the tungstate oxide electrodeposition:

In the tungsten oxide deposition, the perchloric acid is the acidic agent. For this reason, it was necessary to run perchloric acid alone in a cyclic voltammetric experiment at the same pH as the peroxyditungstate solution (pH= 1.4), so as to be able to differentiate their behavior when mixed together.

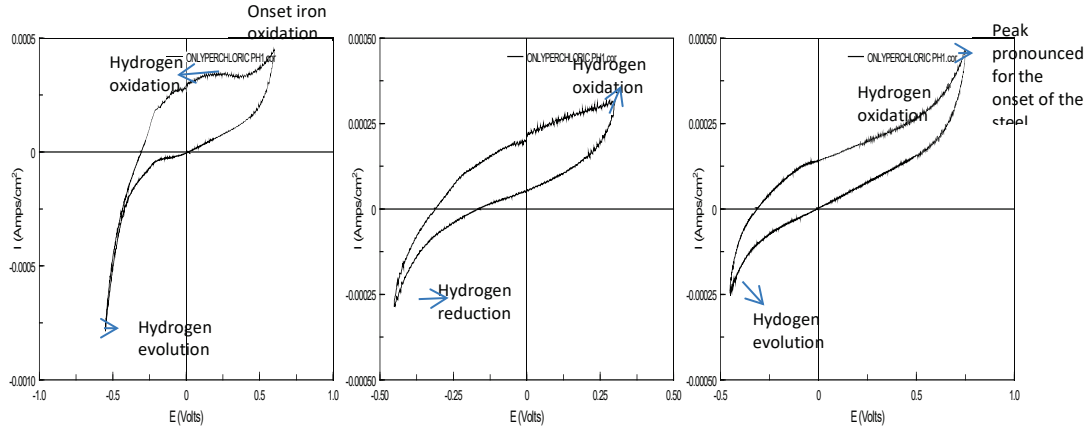

Figure 14. Cyclic voltammetry curves perchloric acid pH = 1.0, WE: thread, RE: silver chloride, CE: platinum; a. (-0.5 – 0.5) V; b. (-0.4 – 0.255) V; c. (-0.45 – 0.75) V

Curve A, on Figure 14, has three important peaks. The big peak on the upper right shows the onset of iron oxidation. There is another small peak on the upper right that means hydrogen oxidation. The lower peak shows hydrogen evolution. The curve B looks smooth and it mainly shows the hydrogen reduction and oxidation. The curve C shows the same peaks of A but in C the upper right peak is more pronounced for the onset of the steel oxidation.

3.5 Perchloric Acid Stability of the Thread:

It was suspected that the thread was dissolved in the perchoric acid during the cyclic voltammetry. This suspicion lead us to soak the thread into three perchloric acid solutions. The first one with pH=1, the second one with pH=2 and the third one with pH=3.

The threads were weighed and soaked in the different solutions, as shown in Figure 15 . There was no weight change 24 hours. It was found that the thread was very stable in acid solution and does not dissolve.

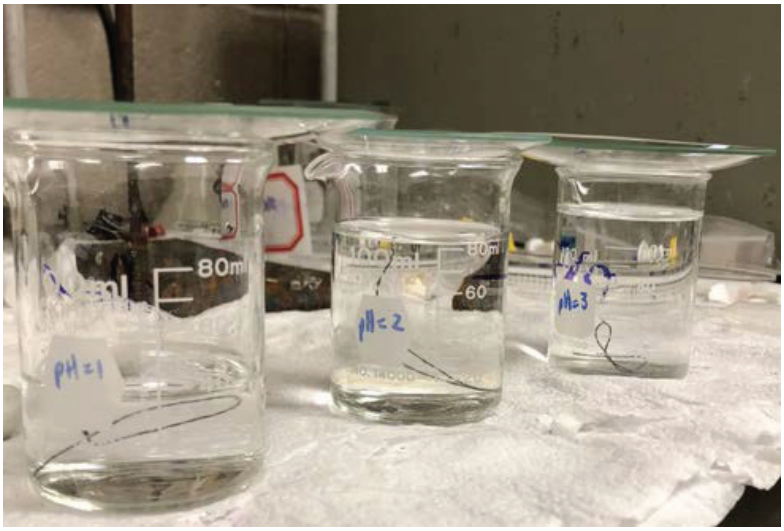

Figure 15. Photograph of three thread samples soaking in three different acidic solutions (pH = 1.0, 2.0 and 3.0) to check for corrosion.

Chapter 4 - Results and Discussion:

4.1 Thread Characterizations:

The substrate for this research is a steel thread, shown in Figure 16 . For this reason, the first step in the research is its characterization by scanning electron microscopy (SEM), energy dispersion spectroscopy (EDX) and thermogravimetric analysis (TGA).

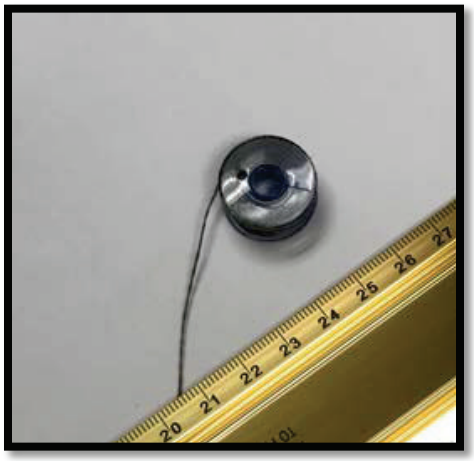

Figure 16. Commercial steel thread.

4.1.1 SEM Results:

The images show many fibers bundled with each other as expected. Each fiber's diameter is around 10 μm, as shown in Figure 17.

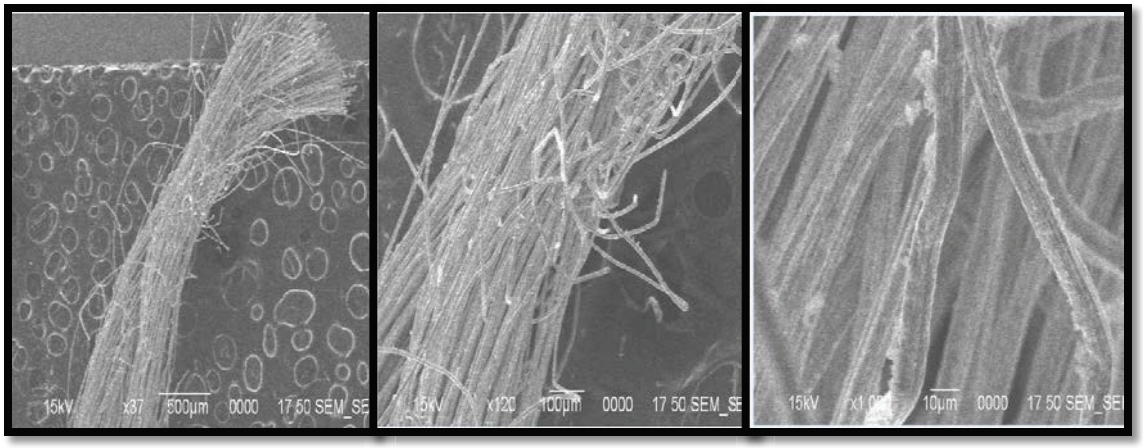

a b c

Figure 17. a. SEM of the thread at low magnification (magnification: 37x); b. SEM of the thread at intermediate magnification (magnification: 120x); c. SEM of the thread at high magnification (magnification: 1000x).

4.1.2 EDX Results:

The EDX results shown in Figure 18 confirm the fact that the thread could be made of steel. Steel is an alloy of iron, carbon and other elements.

The one surprising element is boron. It could be incorporated in order to improve the hardenability. “Hardness is resistance to penetration. Hardenability describes how deep the steel may be hardened upon quenching from high temperature. The depth of hardening is an important factor in a steel part’s toughness” (15). The effect of boron is evident even in low concentrations.

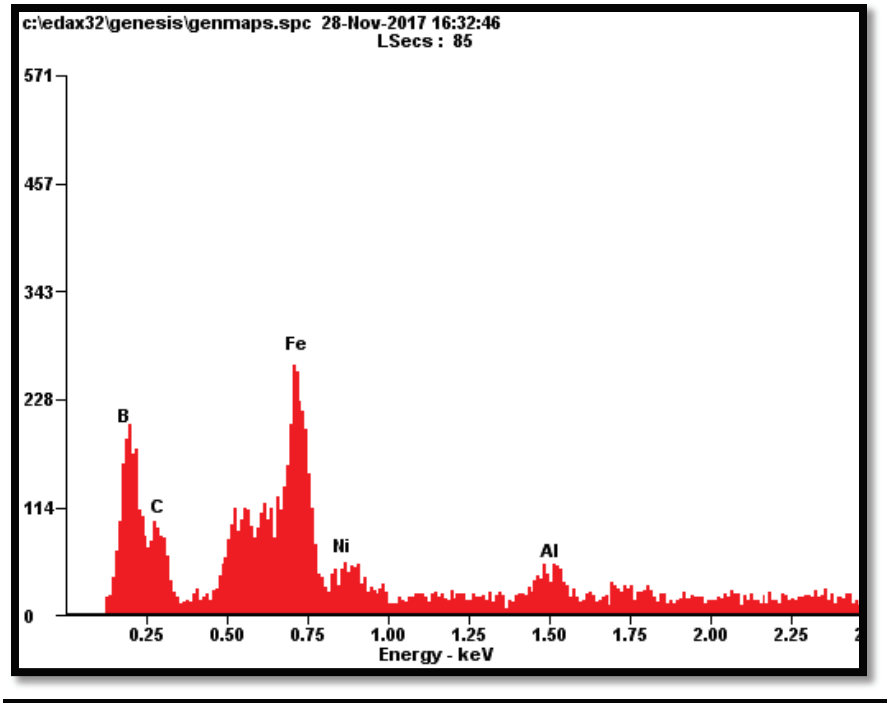

Figure 18. EDX Thread results

4.1.3 Thermogravimetric Analysis (TGA):

Thermogravimetric analysis will help to determine how much organic and inorganic material is present in the thread sample and to evaluate the material's thermal stability. Results are shown in Figure 19, where the weight loss thermogram for the steel thread is plotted along with a sample of stainless steel wire.

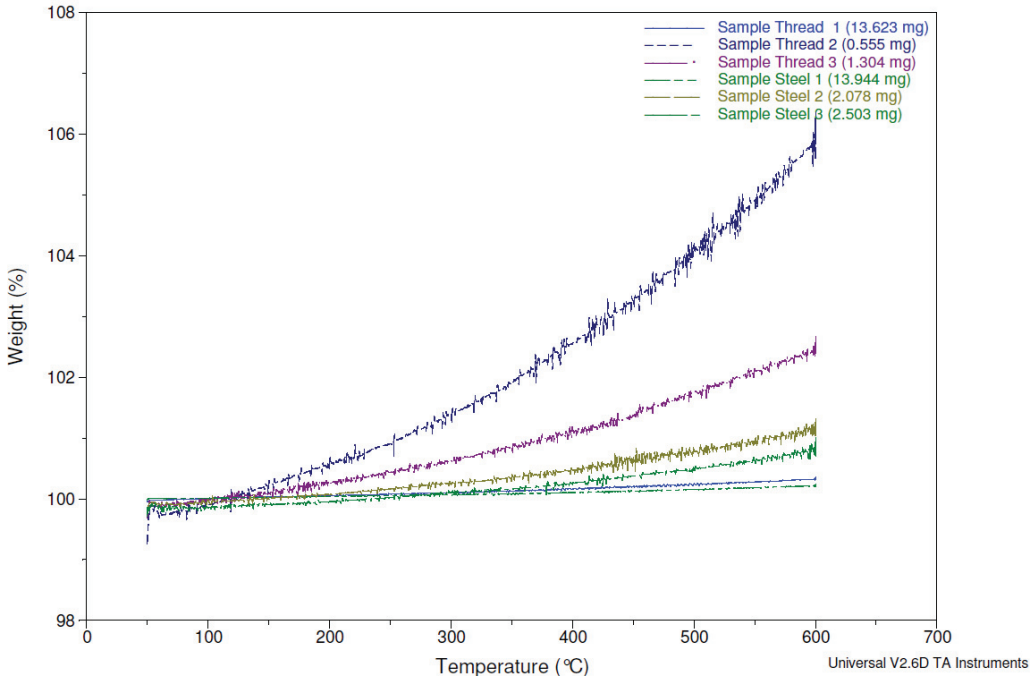

Figure 19. TGA Results, commercial steel thread vs stainless steel wire

The largest thread and stainless steel wire samples tend to be more stable with temperature. These are the samples named Thread 1 and Steel 1. The reason of this behavior is associated with the relationship between the surface area and volume of the sample. The TGA responsiveness increases as the relation between surface area over volume increases. In general, the TGA results for the steel thread show that the sample is very stable with temperature. The lines are nearly in a scale from 0 to 100%. Even though there is weight gain in all the figures, it is very small, and could be associated with base line drift and trace amounts of oxygen in the heating chamber, which cause oxidation. There are no pyrolysis reactions or other bond breakage during the heating. According to these results, it could be said that the thread is composed of bundled metallic fibers without any organic binder. Comparing the thread TGA results to those obtained for the stainless steel wire, similar weight gain behavior was observed. It means

the stainless steel wire and the conductive thread are very similar and stable materials, as it were supposed.

4.2 Approach I Results:

4.2.1 Stainless Steel Strip Electrode:

WO_3 electrodeposition and cyclic voltammetry were performed using a stainless steel strip as electrode. Several pieces were tested. Voltammetric behavior of the steel electrode in the plating solution is shown in Figure 20a. The function in the CorrWare electrochemical software running the PAR 273A potentiostat was Potentiostatic. In this type of experiment, a constant potential is applied. It monitors the current as a function of time. The current-time curve for WO_3 deposition is shown in Figure 20b.

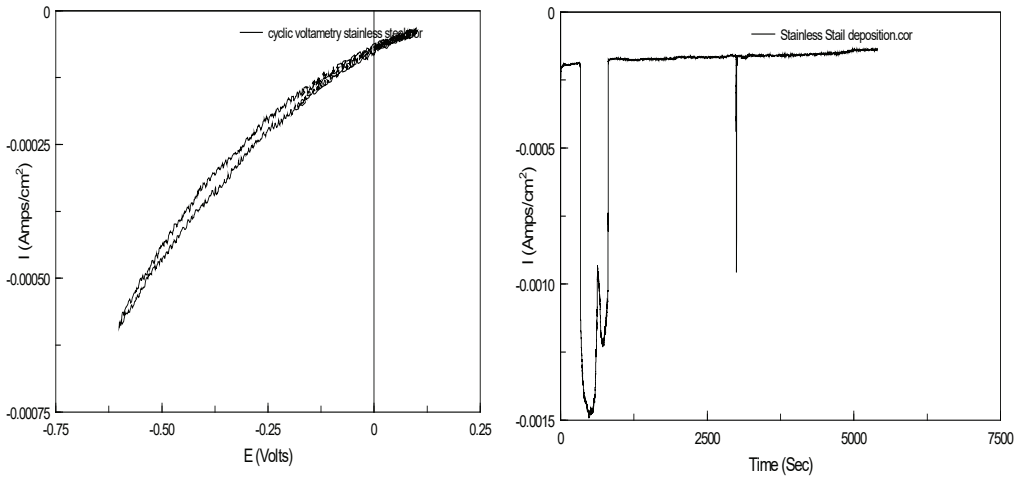

a b

Figure 20. a. Cyclic voltammetry curve for stainless steel strip electrode, RE: silver chloride, CE: graphite, peroxyditungstate / perchloric acid electrolyte; b Potentiostatic electrodeposition curve, for 1.5 hour; -0.5 V; same conditions as in a.

The cyclic voltammetric curve did not resemble the thread cyclic voltammetry. For the stainless steel electrode, the reduction peak for tungsten oxide is not clear around -0.5 V and curve b (electrodeposition) is very noisy due to bubbles coming from peroxide decomposition.

The SEM and EDX results are shown in Figure 21, Figure 22 and Figure 23.

Sample 1:

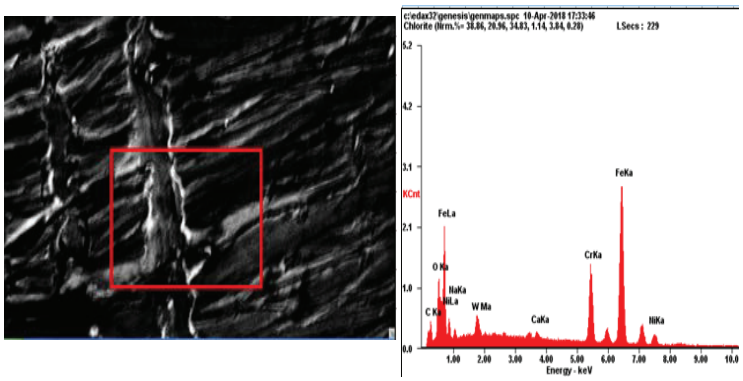

Element	Wt%	At%
CK	07.19	23.89
OK	05.94	14.80
NaK	01.29	02.23
WM	05.74	01.25
CaK	00.73	00.73
CrK	15.56	11.93
FeK	57.37	40.97
NiK	06.18	04.20
Matrix	Correction	ZAF

Figure 21. Stainless steel sample 1 results

Sample 2:

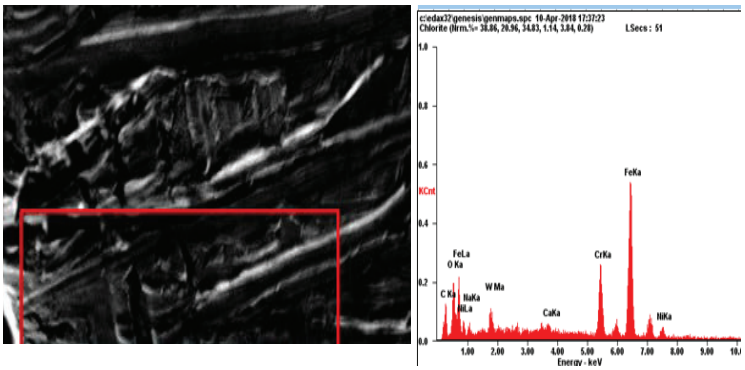

Element	Wt%	At%
CK	11.06	33.40
OK	05.85	13.25
NaK	01.84	02.90
WM	06.64	01.31
CaK	00.79	00.72
CrK	13.96	09.73
FeK	54.30	35.26
NiK	05.56	03.44
Matrix	Correction	ZAF

Figure 22. Stainless steel sample 2 results

Sample 3:

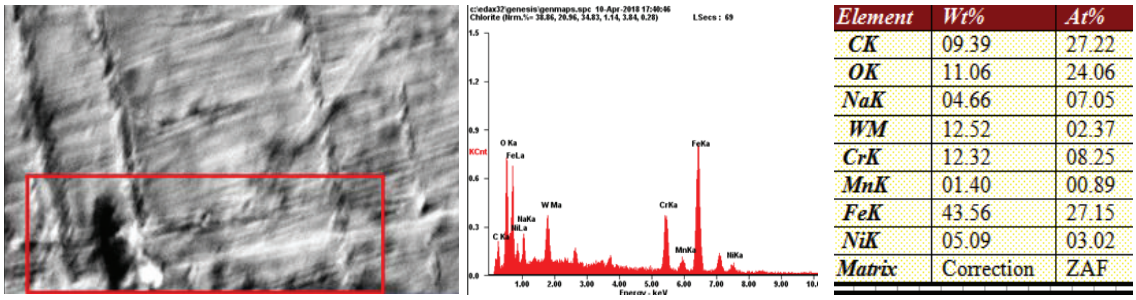

Element	Wt%	At%
CK	09.39	27.22
OK	11.06	24.06
NaK	04.66	07.05
WM	12.52	02.37
CrK	12.32	08.25
MnK	01.40	00.89
FeK	43.56	27.15
NiK	05.09	03.02
Matrix	Correction	ZAF

Figure 23. Stainless steel sample 3 results

The micrographs do not show the WO_3 coating. The images only show the stainless steel morphology.

The EDX results are summarized in Table 1.

They show low but uniform concentrations of tungsten on the electrode. The atomic percentage results do not agree with the expected stoichiometry (for every atom of tungsten, there are three atoms of oxygen).

Table 1. EDX elemental analysis for WO_3 on stainless steel; Approach I

summary of results

	Sample 1		***Sample 2***		***Sample 3***	
	(Weight %)	***(Atomic %)***	***(Weight %)***	***(Atomic %)***	***(Weight %)***	***(Atomic %)***
O	5.94	14.8	5.85	5.85	11.06	24.06
W	5.74	1.25	6.64	1.31	12.52	2.35

Photoelectrochemistry tests were not run for the WO_3 film deposited on stainless steel strip via approach I due to the fact that the strip did not have the expected properties. The negative results on the WO_3 strip was evidence that it was necessary to try another procedure for the coating. It will be named approach II.

4.2.2 Cyclic Voltammetry - Tungsten Oxide electrodeposition on a Thread

The temperature of the electrodeposition experiment was 25 °C; the applied voltage was -0.50 V vs. silver chloride (reference electrode), in a conventional single compartment cell, with a three-electrode setup, consisting of a steel thread electrode (working electrode), silver chloride electrode (0.22 V – reference electrode) and a platinum foil (100 mm^2 surface area – counter electrode).

Voltammetric results for steel thread in the plating solution are shown in Figure 24.

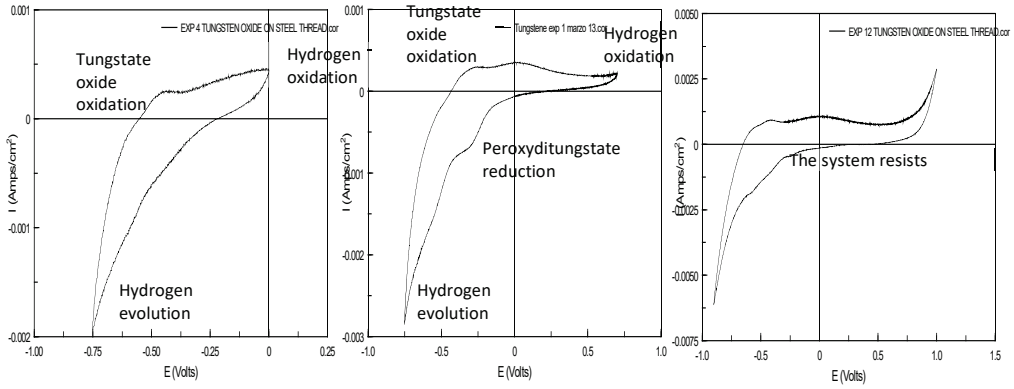

a b c

Figure 24. Cyclic voltammetric curves for WO_3 deposition on steel thread, RE: silver chloride, CE: Platinum, peroxyditungstate/perchloric acid electrolyte; potential ranges: a. (-0.75 – 0.0) V; b. (-0.75 – 1.0) V; c. (-0.75 – 0.75) V

There is a peak around -0.5 V (in all curves), that suggests the reduction of peroxyditungstate to tungsten oxide. Curve A has three peaks. The big peak on the upper right shows hydrogen oxidation. There is another small peak on the upper right, around -0.5 V that could be tungsten oxide oxidation and the lower peak shows hydrogen evolution. Curve B is similar to A but it has an additional lower peak around -0.4 V that could be associated with peroxyditungstate reduction. Curve C shows that the system resists oxidation very well because it needs high positive potential for the oxidation peak.

The cyclic voltammetric peak around -0.5 V and the blue color of the thread are signs of the presence of tungsten oxide. A photograph of blue-coated thread is shown in Figure 25.

Figure 25. Blue color on steel thread after WO_3 deposition.

4.2.3 Electrodeposition via Approach I

The electrodeposition was run at -0.5 V vs silver chloride reference electrode. The function in the CorrWare electrochemical software running the PAR 273A potentiostat was Potentiostatic. In this type of experiment, a constant potential is applied. It monitors the current as a function of time. The potentiostatic current-time curve for WO_3 deposition on steel thread via approach I is shown in Figure 26.

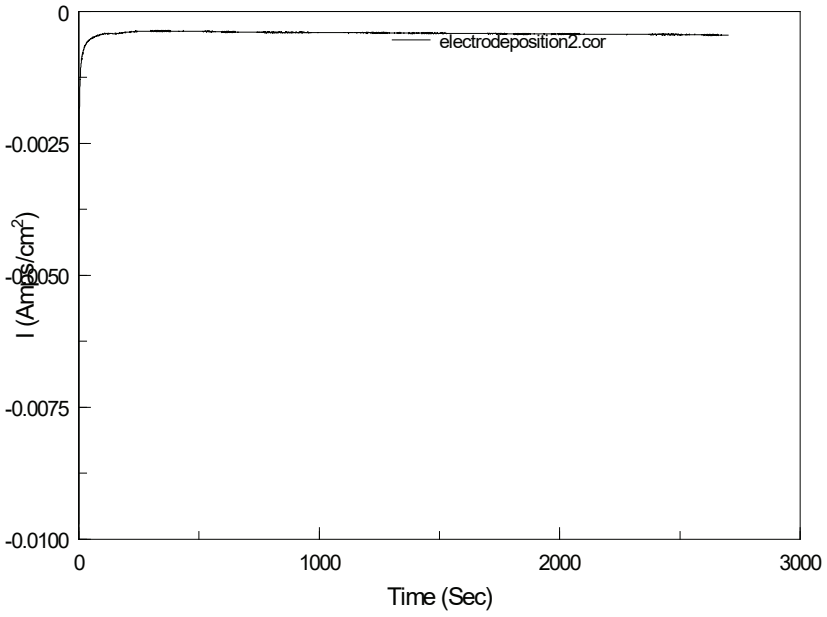

Figure 26. Potentiostatic curve for tungsten oxide electrodeposition (45 minutes) on steel thread.

The curve was very smooth, suggesting a steady deposition process. However, the coating was very thin and could not be observed via naked eye.

There was a problem with the electrolyte. After the electrodeposition, the solution turned cloudy and a white precipitate appeared on the bottom. It was necessary to prepare more fresh solution for continuing other electrodepositions, it is shown on

Figure 27 below. Peroxytungstates are thermodynamically unstable and are prone to hydrolysis and condensation (2), (16).

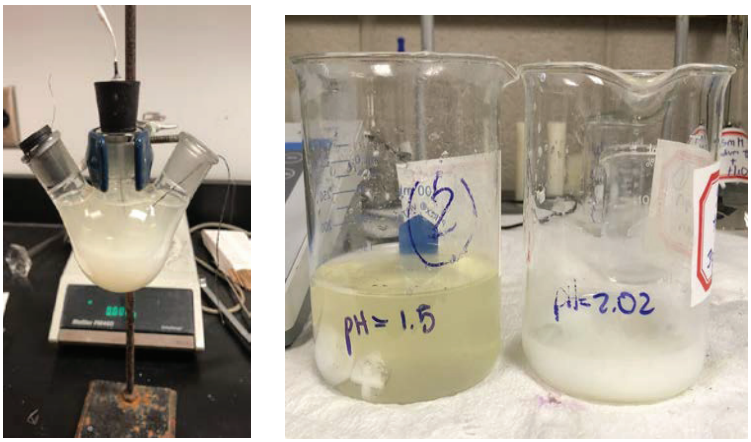

Figure 27 .Decomposition of the Approach I electrolyte

There was another electrodeposition; it lasted 1.5 hours, as shown in Figure 27. However, in this experiment the solution of peroxyditungstate did not reach a 7.6 pH in its preparation because it took a while (10 days) and it was necessary to check if the solution was viable before the end of 10 days. In the first experiment mentioned before (4.2.2 Cyclic Voltammetry - Tungsten Oxide electrodeposition on a Thread), the solution reached 7.6 pH in the peroxotunstate reaction, but in this second experiment, it only reached pH 4.1. The fact that the higher pH was not reached may mean that the reaction was not finished and there was still a lot of hydrogen peroxide, creating too much bubbling. The curve, on Figure 28, has too much noise due to bubbling off the electrode surface during the electrodeposition. It could be associated with the excess of hydrogen peroxide decomposition instead of tungsten oxide electrodeposition.

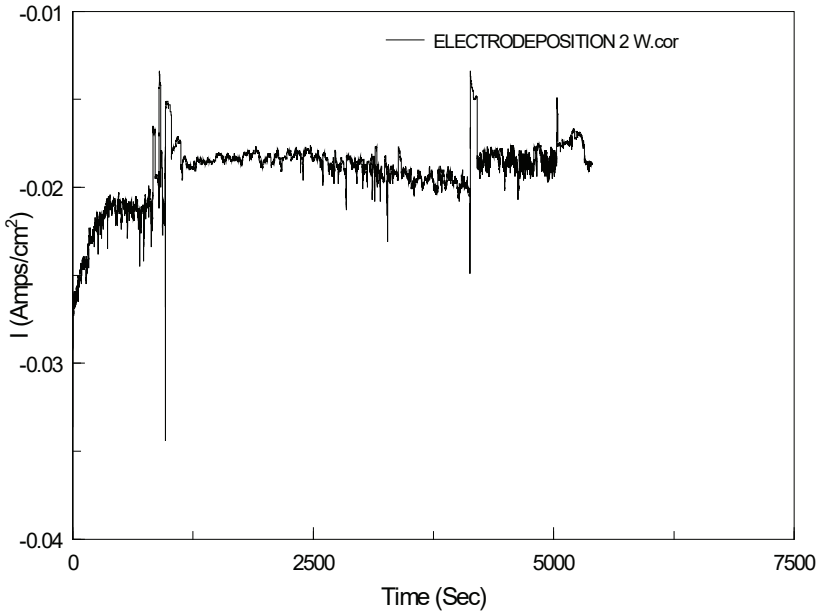

Figure 28. Potentiostatic curve – tungsten oxide electrodeposition(1.5 hour) on steel thread via Approach I.

4.2.4 SEM – EDX Thread Results

4.2.4.1 Steel Thread without thermal treatment:

Two samples were evaluated; the first one was cleaned before the electrodeposition and the other one was not cleaned.

SEM-EDX results for WO_3-coated threads which had been cleaned before WO_3 deposition are shown in Figure 29.

5.2.4.1.1 Washed Sample:

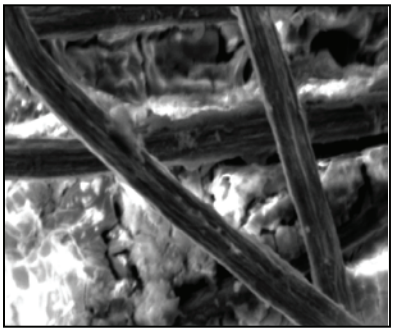

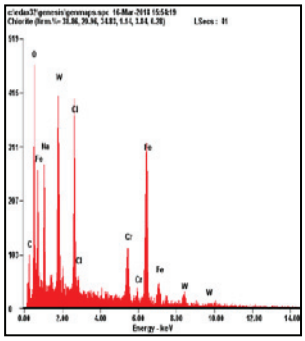

Element	Wt%	At%
CK	09.11	24.45
OK	15.12	30.47
NaK	07.59	10.65
ClK	08.73	07.94
CrK	06.90	04.28
FeK	32.38	18.69
WL	20.16	03.53
Matrix	Correction	ZAF

Figure 29. SEM -EDX data for tungsten oxide electrodeposition on prewashed steel thread

The SEM image Figure 29 shows the coated fibers. The fibers have many cracks. It could be good for the fiber because it could help with the flexibility that the material requires and may render a thermal treatment procedure unnecessary.

Elemental analysis confirmed that tungsten and oxygen are present in the sample, although O is still far in excess of stoichiometry.

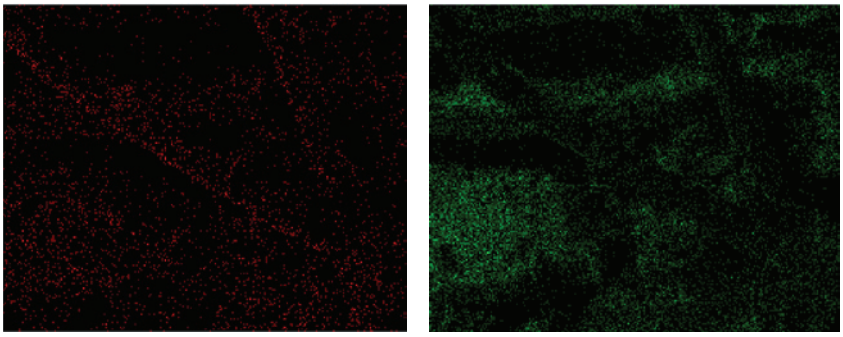

a b

Figure 30 . Elemental mapping of WO_3 electrodeposited on prewashed steel thread; a. Tungsten, b. Oxygen

The elemental maps in Figure 30 show the spatial distribution of W and O. The images indicate that around the thread there are tungsten, oxygen, sodium and potassium

atoms. It was a positive result to know that the oxygen and the tungsten are around the thread.

4.2.4.1.2 Unwashed Sample:

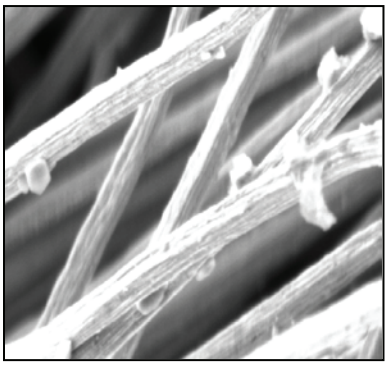

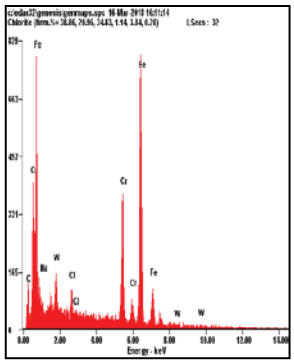

Element	Wt%	At%
CK	07.64	24.33
OK	07.42	17.76
NaK	00.93	01.54
ClK	01.42	01.54
CrK	17.95	13.21
FeK	59.03	40.45
WL	05.61	01.17
Matrix	Correction	ZAF

Figure 31. SEM -EDX data for tungsten oxide electrodeposition on unwashed steel thread

The image in Figure 31 shows coated fibers. However, it does not show cracks around the fibers. It could be because the coating concentration was low, so it is difficult to appreciate the coating morphology. The elemental analysis confirms the fact that the tungsten and the oxygen are present in the sample in low concentrations.

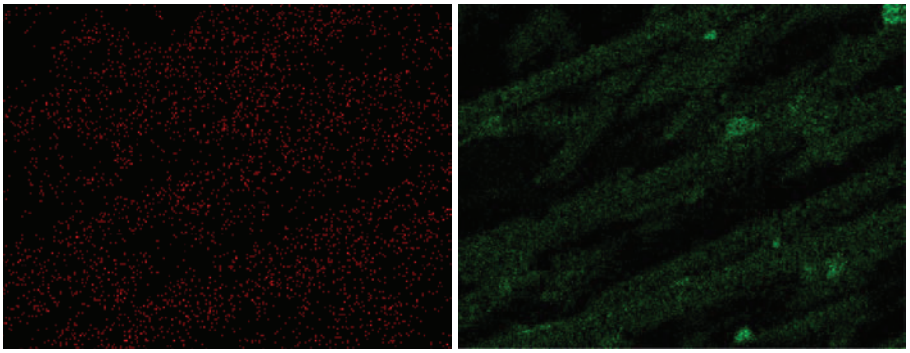

a b

Figure 32. Elemental mapping of WO_3 electrodeposited on unwashed steel thread a. Tungsten, b. Oxygen.

The elemental mapping images in Figure 32 show that the thread is clad with tungsten and oxygen.

4.2.4.2 Steel Thread with thermal treatment:

After the electrodeposition, the sample was heated to 600 °C and later the SEM analysis was done.

4.2.4.2.1 Washed Sample:

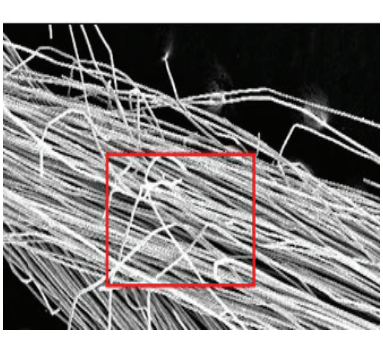

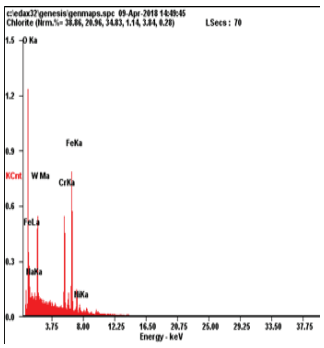

Element	Wt%	At%
OK	15.36	42.64
NaK	01.44	02.78
WM	22.55	05.45
CrK	17.25	14.74
FeK	40.16	31.95
NiK	03.23	02.45
Matrix	Correction	ZAF

Figure 33. SEM -EDX results for tungsten oxide electrodeposition on prewashed steel thread with thermal treatment at 600 ºC (magnification: 80x)

The image in Figure 33 shows the coated fibers. The fibers look disorganized.

4.2.4.2.2 Sample without Washing:

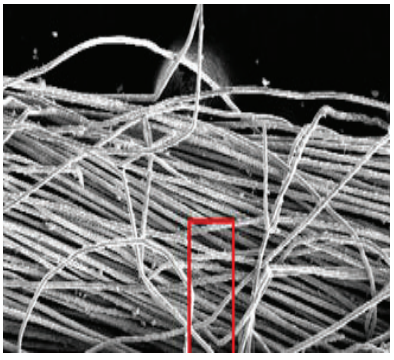

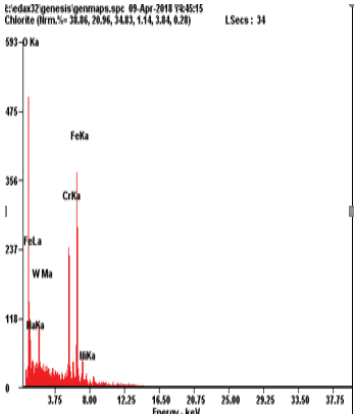

Element	Wt%	At%
OK	13.93	37.27
NaK	01.91	03.56
WM	11.91	02.77
CrK	20.64	16.99
FeK	47.69	36.55
NiK	03.92	02.86
Matrix	Correction	ZAF

Figure 34. SEM–EDX results for tungsten oxide electrodeposition on unwashed steel thread with thermal treatment (magnification: 130x)

The image in Figure 34 for WO_3 electrodeposited and annealed on unwashed thread shows disorganized coated fibers as well.

4.2.5 Summary EDX analysis for steel thread with and without thermal treatment:

Table 2 . Percentage of tungsten found on steel thread via Approach I

as a function of washing and thermal treatment

	Without Thermal Treatment				***With Thermal Treatment***			
	Wt% (Washed)	***At % (Washed)***	***Wt% (Unwashed)***	***At % (Unwashed)***	***Wt% (Washed)***	***At % (Washed)***	***Wt% (Unwashed)***	***At % (Unwashed)***
O	15.12	30.47	7.42	17.76	15.36	42.64	13.93	37.27
W	20.16	3.53	5.61	1.17	22.55	5.45	11.91	2.77

Table 2 above shows that the washed and the heated samples have more tungsten around the fibers. However, it does not mean that tungsten is present in the form of tungsten oxide. In fact, the atomic percentage results from the EDX do not agree with the stoichiometry (per every atom of tungsten, there are three atoms of oxygen).

4.2.6 Photoelectrochemistry Thread Electrode:

The WO_3 film on stainless steel strip electrode has similar photoelectrochemical behavior to that shown in Figure 35. The graph comes from a research paper entitled, ´´Development of a hydrogen evolving photocatalytic membrane´´. This research worked on a photocatalytic membrane with two semiconductors layers, which combine

their photopotentials to obtain a water-splitting voltage. The membrane had to have compatible deposition steps in order to build n-type WO_3 and p-CdTe layers on opposite sides of a steel sheet . Finally, the membrane produced a 0.8 V photovoltage (6). The main idea of this research is to create a coating steel thread with a similar photoelectrochemistry, in which -0.5V photovoltage was measured for the onset of oxygen evolution, under illumination.

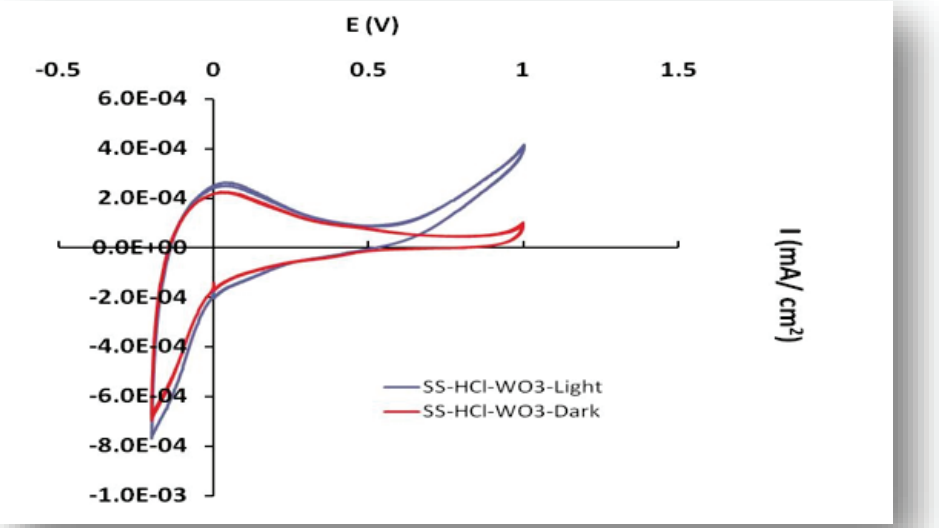

Figure 35. O_2 evolution and Photochemistry of stainless steel substrate -HCl-WO_3 in 0.1 M H_2SO_4. (6)

Once the thread electrode is made, the cyclic voltammetric curve in 0.1 M H_2SO_4 should be close to the stainless steel strip electrode, and follow the following behavior: the peak on the upper right shows water oxidation to oxygen. The upper peak on the left shows hydrogen oxidation on the electrode, and the lower peak on the left shows hydrogen evolution from the sulfuric acid present.

Photoelectrochemistry tests were not run for the stainless steel strip because the strip did not have the expected properties. However, it was run on the stainless steel thread. The result is shown in Figure 36.

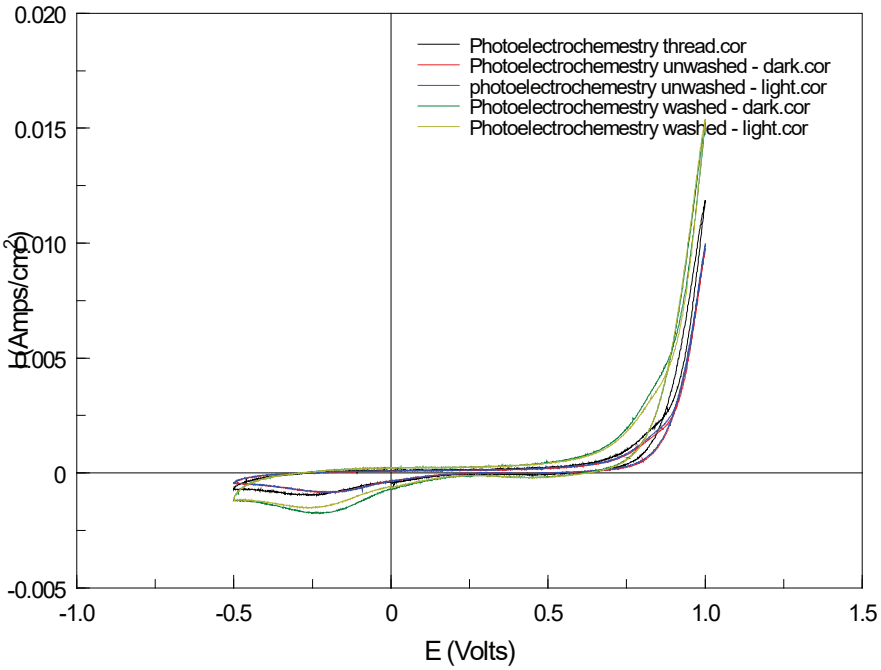

Figure 36. Photoelectrochemistry of WO_3 on steel thread substrate- in 0.1 M H_2SO_4.

The curves do not show a photopotential between light and dark, and it looks very different from the pattern obtained by Rhoden (6). There is no photopotential between the onset of oxygen evolution under illumination and darkness. There is very little evidence of O_2 evolution in most of the voltammograms.

4.2.7 Thermogravimetric Analysis (TGA):

Thermogravimetric analysis (TGA) will help to evaluate the decomposition reactions after the electrodeposition on the thread. It will show the weight change when

the sample begins to decompose; this information is very valuable for the material's applications because it is related to its thermal stability. (2)

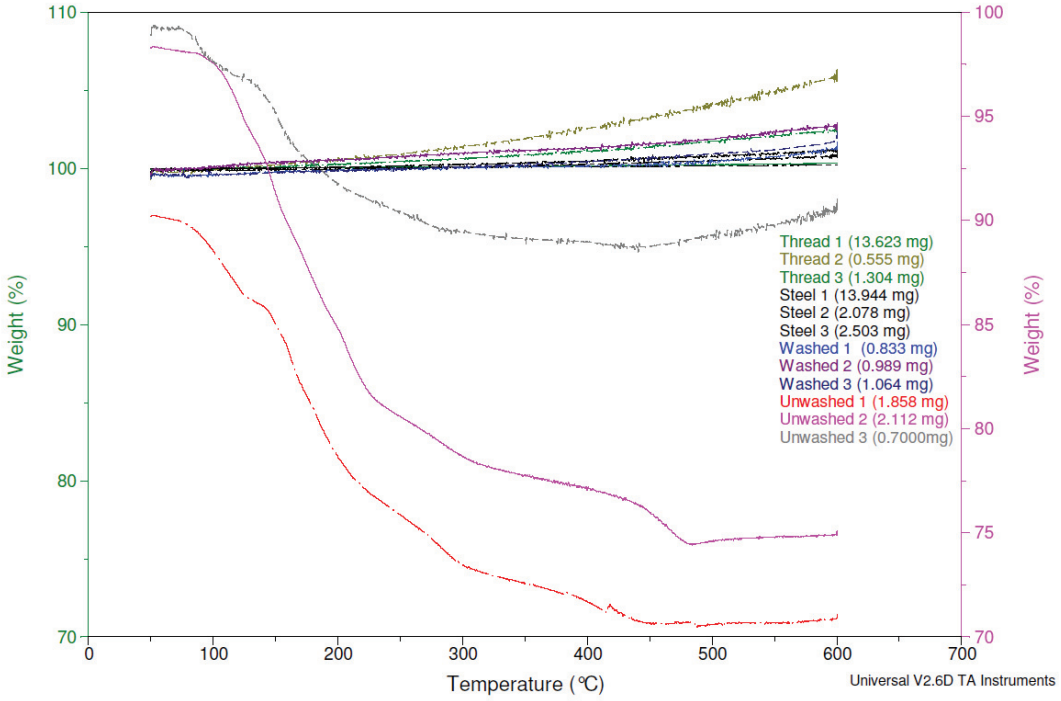

Figure 37. TGA results for washed and unwashed WO_3 – coated and uncoated steel thread

There are four kinds of samples shown in the thermograms, in Figure 37. The naked threads include: Thread 1, Thread 2 and Thread 3. The second kind of samples is stainless steel wire, which includes: Steel 1, Steel 2 and Steel 3. The third kind of samples is washed thread, which is coated with tungsten oxide (dried after electrodeposition) and includes: Washed 1, Washed 2 and Washed 3. The fourth kind of sample is unwashed thread, which is coated with tungsten oxide (dried after electrodeposition), and includes: Unwashed 1, Unwashed 2 and Unwashed 3.

There is weight gain in some curves, and could be associated with base line drift and trace amounts of oxygen in the heating chamber, which caused oxidation of the steel alloy.

All the samples, except for the unwashed samples, tended to be very stable at high temperature. The unwashed samples tended to lose weight (25% loss, on average). This behavior could be associated with the water of hydration and peroxides eliminated by the heat. Another important factor could be the relationship between the surface area and volume of the sample, because TGA responsiveness increases as the relation between surface area and volume increases.

These TGA results complement the EDX elemental analysis results, which suggest that the cleaning procedure, with thermal treatment after the electrodeposition, will improve the tungsten oxide coating.

4.3 Approach II Results:

Approach II tries to increase the thickness of the coating in order to improve the photoelectrochemistry results. Previous research (6) and Approach I show that washing and heating help to enhance the coating, so in Approach II, all the samples were heated and washed.

4.3.1 Stainless Steel Strip Electrode :

The comparison pattern is the same one that was used in Approach I and the results obtained are the following shown in Figure 38.

Cyclic Voltammetry:

Cyclic voltammetric results for stainless steel strip electrodes coated with WO_3, prepared via Approach II, are shown in Figure 38.

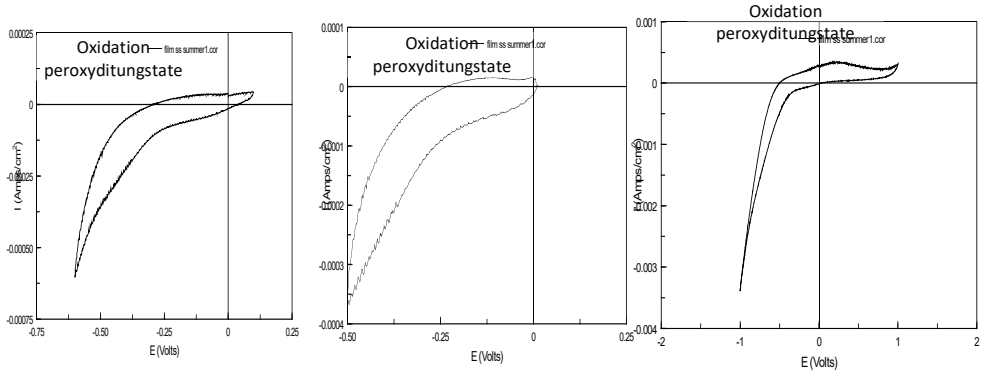

a b c

Figure 38. Cyclic voltammetry curves for stainless steel strip electrode. RE: silver chloride, CE: graphite, $W_2O_{11}^{-2}/HClO_4$ electrolyte. a. (-0.60 – 01.) V; b. (-0.50 – 0.01) V; c. (-1.00 – 1.00) V

The cyclic voltammetric curves in Figure 38 are similar to the ones obtained for the thread with Approach II. There is a peak around -0.4V that suggests the reduction of peroxoditungstate ion to tungsten oxide. For the thread electrodes, this peak was closer to -0.5 V.

Electrodeposition:

A current vs time curve for WO_3 electrodeposition on stainless steel is shown in the Figure 39.

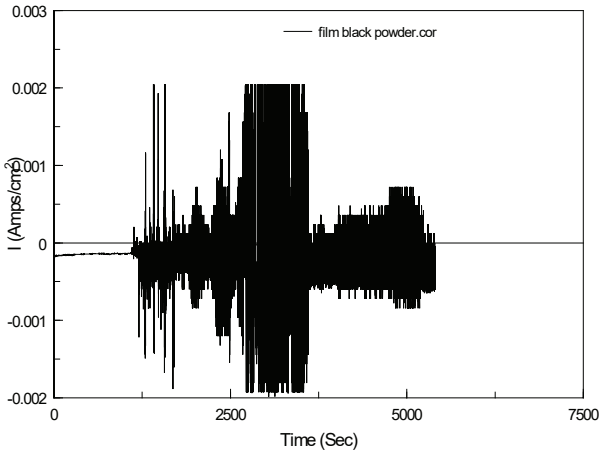

Figure 39. Current vs time curve for WO_3 electrodeposition on stainless steel with Approach II

The electrodeposition shown in Figure 39 was noisy. It is impossible to derive information from it. Once the electrodeposition was done, the stainless steel electrode was washed with ethanol and DI water, and then allowed to air dry. After that, it was heated to 450°C. Figure 40 shows how it looked after the thermal treatment. It still had some blue areas on it.

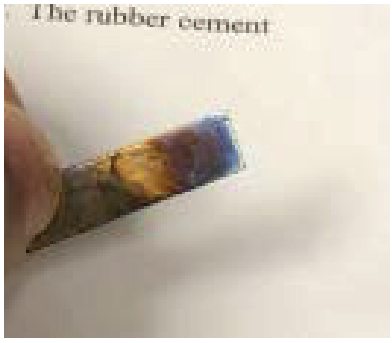

Figure 40. WO_3- coated stainless steel electrode after thermal treatment

SEM and EDX results, Approach II:

Three steel strip samples underwent electrodeposition of WO_3, and the results are shown on Figure 41, Figure 42 and Figure 43:

Sample 1:

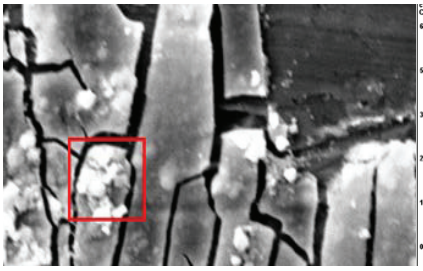

Element	Wt%	At%
OK	21.14	63.80
NaK	03.18	06.68
AlK	00.19	00.34
CaK	00.69	00.83
CrK	13.07	12.14
WL	61.73	16.22
Matrix	Correction	ZAF

Figure 41. Sample 1, tungsten oxide electrodeposition on the strip (SEM -EDX results) (magnification: 6500x)

Sample 2:

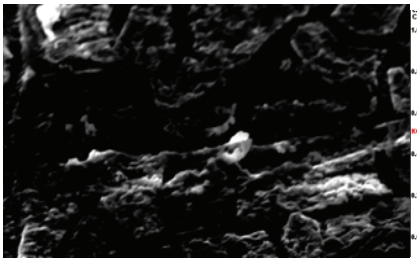

Element	Wt%	At%
OK	24.92	63.52
NaK	06.40	11.35
AlK	00.46	00.69
CaK	00.79	00.80
CrK	15.43	12.10
WL	52.01	11.54
Matrix	Correction	ZAF

Figure 42. Sample 2, tungsten oxide electrodeposition on the strip (SEM -EDX results)

Sample 3:

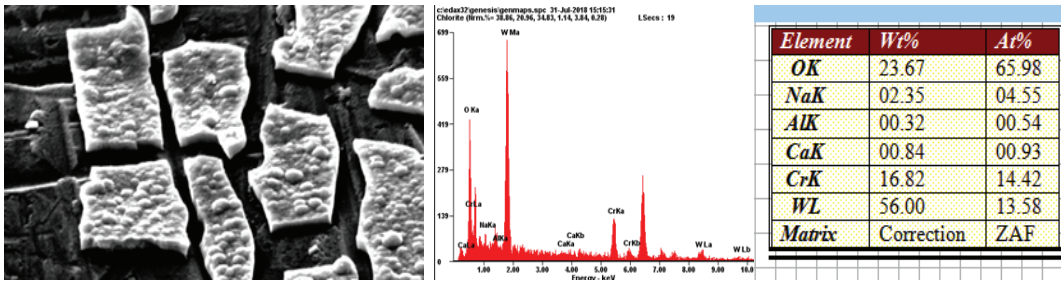

Figure 43 . Sample 3, tungsten oxide electrodeposition on the strip (SEM -EDX results)

The images (Figure 41, Figure 41, Figure 42) show that the coating is formed by a series of amorphous shapes that are separated one from the other. The morphology is similar to the previously analyzed pattern in Approach I. The thickness of the tungsten oxide on steel strip was about 1µm, which was measured by cross-sectional SEM observations.

Table 3. EDX elemental analysis for WO_3 on stainless steel strips, Approach II

	Sample 1		***Sample 2***		***Sample 3***	
	(Weight %)	***(Atomic %)***	***(Weight %)***	***(Atomic %)***	***(Weight %)***	***(Atomic %)***
O	21.14	63.80	24.92	63.52	23.67	65.98
W	61.73	16.22	52.01	11.54	56.00	13.58

The EDX results show uniform concentration of tungsten on the different samples. The table above shows the samples have an average of 56.58 wt% of tungsten. The atomic percentage results are not very close to the actual ratios for WO_3, but it is an

improvement if it is compared with Approach I. It looks like a 50% excess of O, which may be due to steel oxidation during annealing.

Photoelectrochemistry of WO_3 on steel strip results:

The curves in Figure 44 look different than the corresponding curves mentioned in Approach I.

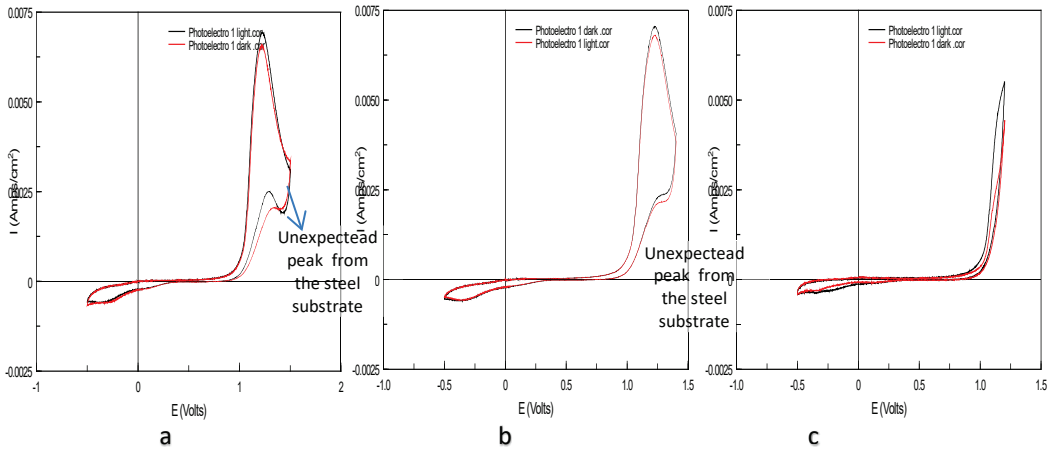

Figure 44. Photoelectrochemistry of stainless steel substrate-WO_3 in 0.1 M H_2SO_4, in three different voltage ranges (stainless steel strip as WE)

The curves do not show appreciable photopotential between light and the dark, but nevertheless look very different from the voltammograms that were obtained in Approach I (4.2.6 Photoelectrochemistry Thread Electrode:). When the positive potential is swept above 1.3 V, there is an unexpected reduction peak on the return sweep from the steel substrate, which can be seen in curves a and b.

The photoelectrochemistry results with Approach II were not successful, so it was necessary to determine what was causing the problem. The stainless steel strip was used

for that purpose. It was cleaned, subjected to WO_3 electrodeposition, and annealed, and it was observed under SEM in every step to know where the mistake was. The SEM images on Figure 45 show the following:

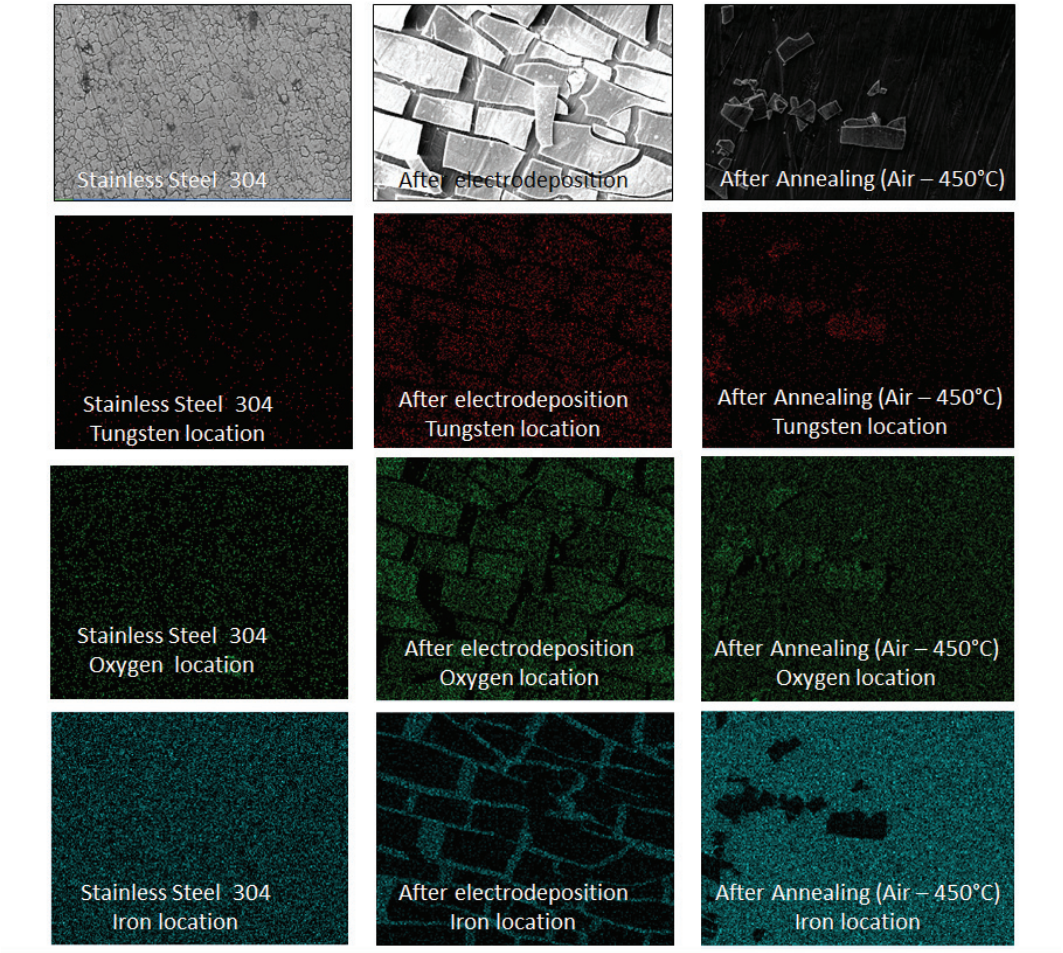

Figure 45. Electron micrographs of WO_3 film on stainless steel strips at various stages of fabrication

The left column corresponds to the stainless steel after the cleaning process. It is mainly covered by iron (blue dots). The center column shows that once the electrodeposition is done, the tungsten oxide covers most of the surface. It consists of irregular shapes or patches on the substrate with cracks around them. In addition, the

oxygen atoms locations match with the tungsten atoms locations, which could indicate the presence of the tungsten oxide molecule. The iron is in the cracks. Until that point the results are as expected, but after the annealing with air, a surprising but also negative results was observed. These results are in the right column, which shows that the tungsten is mostly lost; the film does not have good adhesion to the substrate. These results led to performing the annealing treatment under argon atmosphere.

4.3.2 Cyclic Voltammetry - tungsten oxide electrodeposition on a steel thread:

The temperature of the electrodeposition experiment was 25 °C; the applied voltage was -0.50 V vs. silver chloride (reference electrode), in a conventional single compartment cell, with a three-electrode setup, consisting of a steel thread electrode (working electrode), silver chloride electrode (0.22 V vs NHE) and graphite (counter electrode). The following results were obtained when the cyclic voltammetry was run, (Figure 46):

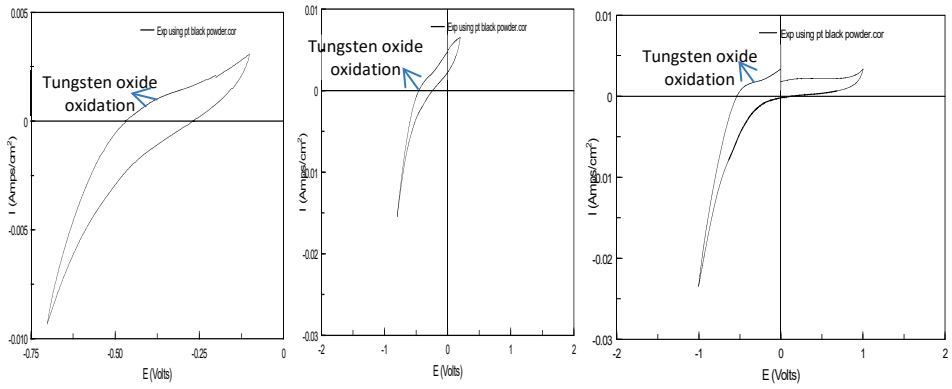

a b c

Figure 46. Cyclic voltammetry curves for steel thread in $W_2O_{11}^{-2}$/$HClO_4$ solution, WE: thread, RE: silver chloride, CE: graphite, (tungstate oxide from peroxotungstate); a. (-0.75 – -0.1) V; b. (-1.0 – 0.5) V; c. (-1.0 – 1.0) V

There is a cathodic wave around -0.5 V, that suggests the reduction of peroxotungstate to tungsten oxide.

The thread's color turned blue when the voltage was negative and went back to gray when the voltage was positive. This was a positive sign of the tungsten oxide presence. Figure 47 shows the blue color on the thread when the voltage was negative.

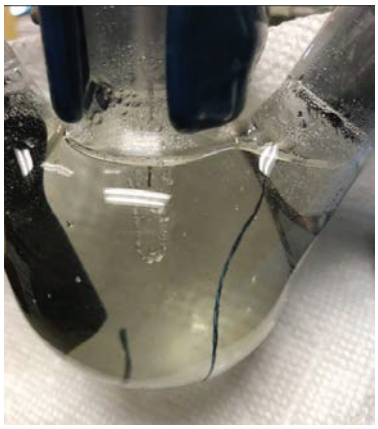

Figure 47. Blue color on a steel thread electrode during $W_2O_{11}^{-2}$ electroreduction

4.3.3 Electrodeposition:

The electrodeposition was run at -0.5 V vs silver chloride reference electrode. The resulting potentiostatic current-time curve is shown in Figure 48:

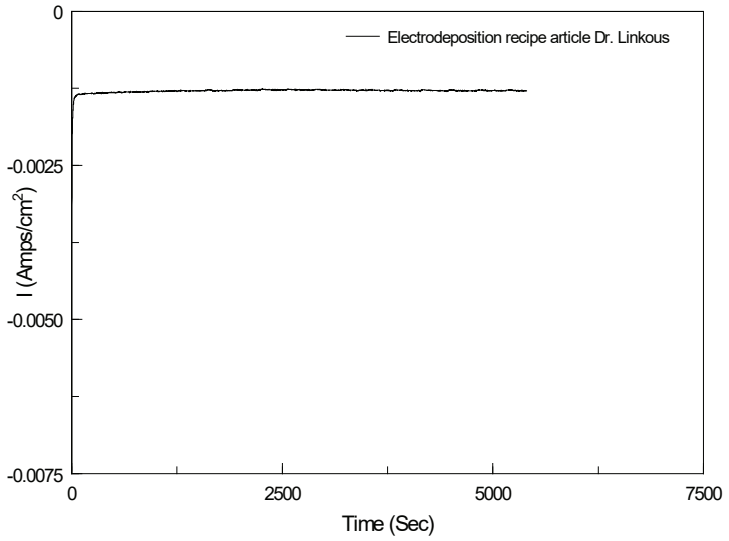

Figure 48. Potentiostatic curve for tungsten oxide electrodeposition on steel thread (1.5 hour deposition time)

According to the electrodeposition curve, there is 9.72 mg of tungsten oxide around the 4 cm long thread (Equation 1. Film Thickness). The curve was very smooth, suggesting a successful process. In theory, the film thickness is approximately 11 µm. Once the electrodeposition was done, the thread recovered its initial gray color, as shown in Figure 49.

Figure 49. Steel thread electrode after WO_3 electrodeposition, removal from solution and drying

4.3.4 SEM – EDX Thread Results

Figure 50, Figure 51 and Figure 53 were taken after the electrodeposition and heating (nitrogen atmosphere – 600 °C) with Approach II solution. All the samples were heated and washed.

Sample 1:

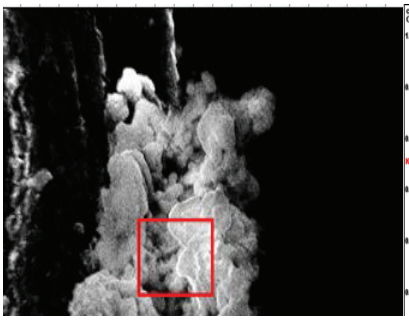

Element	Wt%	At%
OK	31.68	73.43
NaK	02.23	03.59
AlK	00.74	01.02
CaK	08.76	08.10
CrK	04.77	03.40
WL	51.82	10.45
Matrix	Correction	ZAF

Figure 50. Sample 1. Tungsten oxide electrodeposition on steel thread and heated to 600 °C under Ar (SEM-EDX results)

Figure 50 shows the WO_3 coating for Sample 1. It looks amorphous. The amount of tungsten (weight percentage) increased with respect to Approach I. In Sample 1, the atomic percentages for W and O were not very close to the correct stoichiometry.

Sample 2:

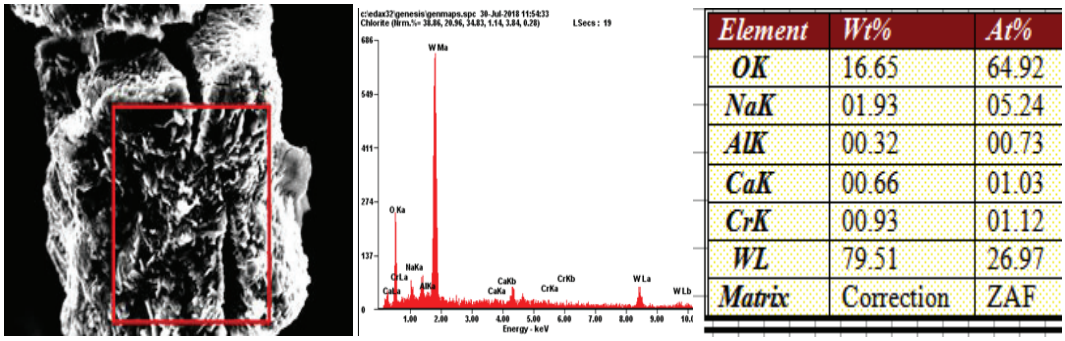

Element	Wt%	At%
OK	16.65	64.92
NaK	01.93	05.24
AlK	00.32	00.73
CaK	00.66	01.03
CrK	00.93	01.12
WL	79.51	26.97
Matrix	Correction	ZAF

Figure 51. Sample 2. Tungsten oxide electrodeposition on steel thread (SEM -EDX results) (magnification: 4500x)

The micrograph of Sample 2 in Figure 51 shows the WO_3 coating around the steel thread. The coating has cracks around the fibers and it looks amorphous; its surface is not very flat. The amount of tungsten (weight percentage) increased with respect to Approach I. In this sample 2, the atomic percentages are closer to the stoichiometric values. In fact, in this instance, the O-content is in deficit with respect the stoichiometry, i.e., if W is present in 26.97 atomic percent, the O should be 80%, which is not possible. Since Sample 2 is closer to the expected results, elemental maps were generated to find the atoms´ locations. These are shown in Figure 52.

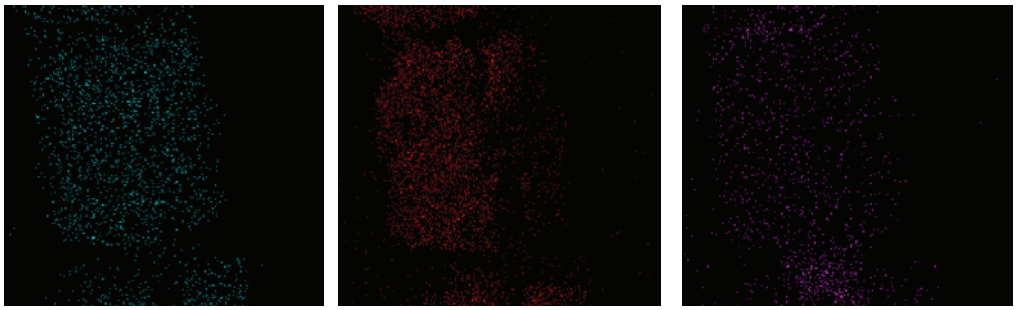

a b c

Figure 52. Elemental maps of several elements in Sample 2. a. Tungsten; b. Oxygen and c. Chromium.

The micrographs in Figure 52 show that the tungsten and the oxygen atoms are around the thread, in the coating, while the chromium is in the thread.

Sample 3:

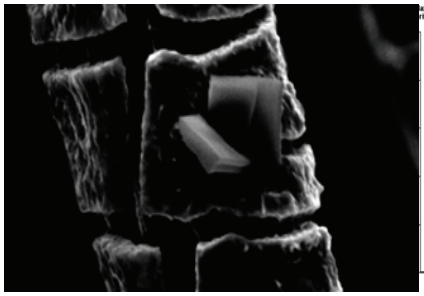

Element	Wt%	At%
OK	19.59	60.49
NaK	05.59	12.01
AlK	00.87	01.60
CaK	01.00	01.24
CrK	07.43	07.06
WL	65.52	17.60
Matrix	Correction	ZAF

Figure 53. Sample 3. Tungsten oxide electrodeposition on the steel thread (SEM-EDX results)

The micrograph for Sample 3 in Figure 53 clearly shows the WO_3 coating. The coating has many cracks around the fiber and its surface is rough. The amount of tungsten (weight percentage) increased with respect to Approach I. In Sample 3, the atomic percentages are closer to the stoichiometric values, with O slightly in excess with

respect to W. Since Sample 3 was close to the expected results, elemental maps were acquired once again.

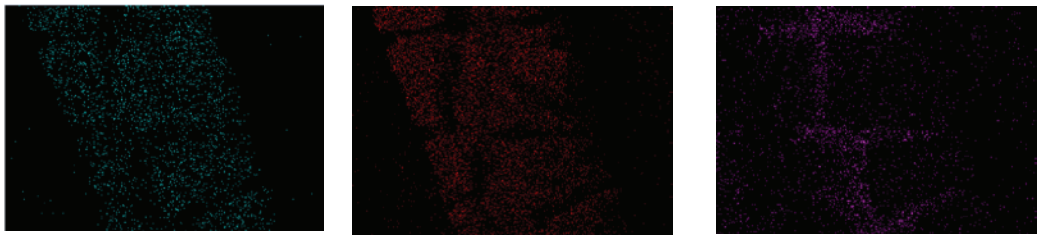

a b c

Figure 54. Elemental maps for WO_3/steel thread, Sample 3. a. Tungsten ; b. Oxygen and c. Chromium

The images above in Figure 54 show that the tungsten and the oxygen atoms are around the thread, within the coating, while the chromium is in the thread.

5.3.4.1 Micrographs of other WO_3/steel thread samples:

Other images of steel deposits on steel thread are shown in Figure 55.

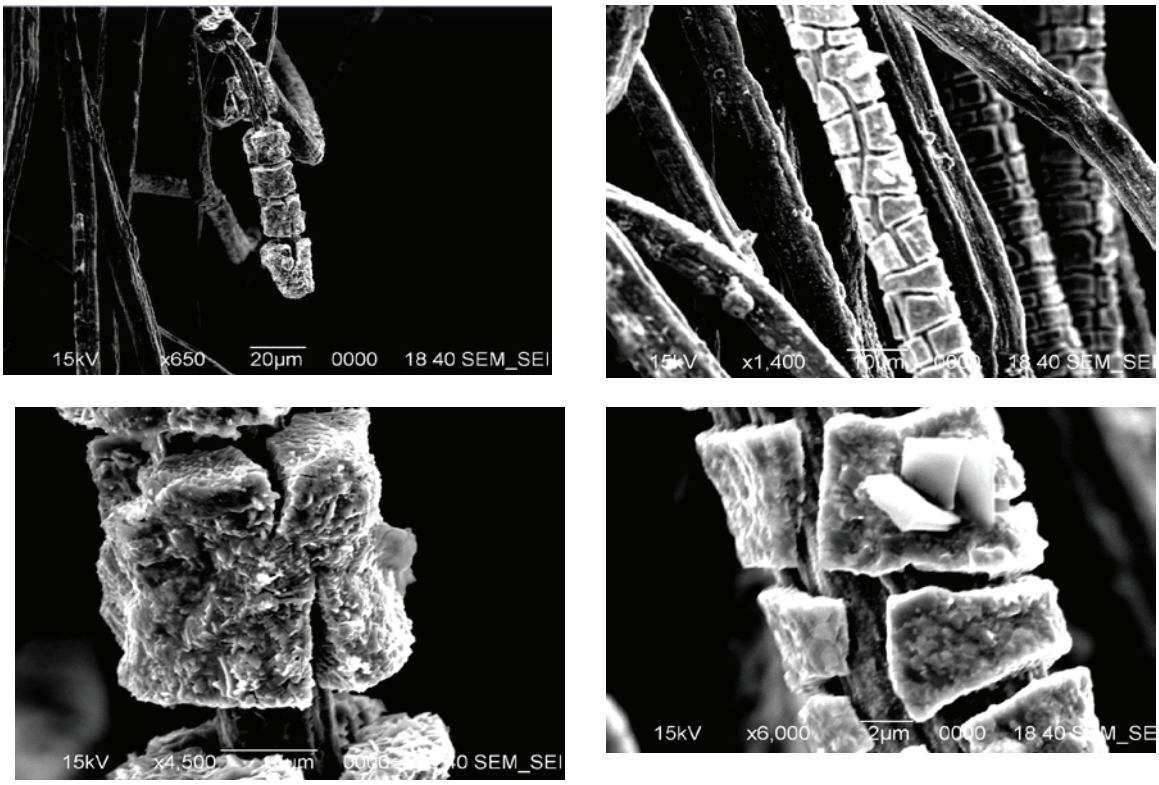

Figure 55. SEM images of WO_3 coatings on steel thread. (Upper left magnification: 650x), (upper right magnification: 1400x), (lower left magnification: 4500x), (lower right magnification: 6000x)

The images in Figure 55 clearly show that the WO_3 coating surrounds the individual fibrils in the thread. The coating is amorphous with a small degree of microcrystallinity, and its surface is rough. The coating has many cracks. Those cracks could help with the flexibility of the thread.

4.3.5 Summary EDX analysis for steel thread:

Table 4. Tungsten/oxygen weight percentage results for WO_3 coatings prepared via Approach II.

	Sample 1		***Sample 2***		***Sample 3***	
Element	***Wt%***	***At%***	***Wt%***	***At%***	***Wt%***	***At%***
O	31.68	73.43	16.65	64.92	19.59	60.49
W	51.82	10.45	79.51	26.97	65.52	17.60

Table 4 shows that the samples have an average of 65.62 wt% of tungsten. This concentration of tungsten is better than what was achieved with Approach I. In addition, the atomic percentage ratio of O to W calculated for the three samples were closer to the stoichiometric values for tungsten oxide (per every atom of tungsten, there are three atoms of oxygen).

However, it does not mean that all of the tungsten is in the tungsten oxide structure, since, the atomic percentage results from the EDX do not exactly match with the WO_3 structure.

4.3.6 Thermogravimetric Analysis (TGA):

Thermogravimetric analysis of samples prepared via Approach II are shown in Figure 56. Samples were taken straight from the electrolyte.

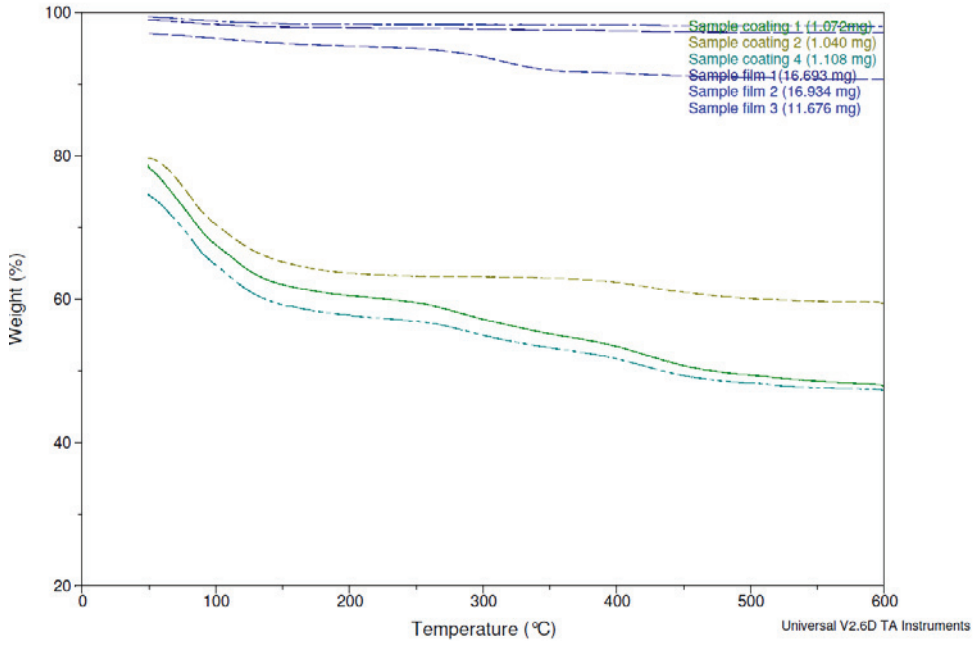

Figure 56. TGA results for WO_3 coatings on steel substrate vs thread, Approach II.

There are two kinds of samples in Figure 56, the coated thread (sample coating 1, 2 and 4) and the stainless steel strip (sample film 1, 2 and 3).

All the stainless steel strip samples tend to be very stable with temperature, but the coated thread samples tend to lose weight (25% loss, on average). This behavior could be associated with the hydrates and peroxides eliminated by the heat.

The relationship between the surface area and volume of the sample is again apparent in these results.

4.4 Approach III

In Approach III, all the electrolyte solutions were purged with argon gas at least 10 minutes before the experiment. The solution was stirred during the electrodeposition

and the annealing process was performed under argon, for 1 hour at either 450 °C or 600 °C. The heat treatment serve the purpose of eliminating hydrates to obtain the desired crystal phase. According to Cotton and Wilkinson, "Post annealing above 400 °C is usually conducted to transform the WO_3.n H_2O to monoclinic WO_3. However, annealing tends to increase the grain size and decrease the porosity of the film" (7). The monoclinic phase has been reported to be the most stable phase at room temperature, so these procedures have the purpose of improving the crystal structure to enhance its photovoltaic properties as well. For the annealing with argon, there is an equilibrium that can be observed with the following:

$$WO_3 \overset{Heat}{\Longleftrightarrow} WO_{3-x} + \frac{x}{2} O_2$$

The presence of heat with argon flow chases away the oxygen. Taking oxygens out of the tungsten oxide lattice, known as vacancy doping, helps to improve the electrical conductivity, which is a desired property for this research application. Tungsten oxide itself is an insulator. In order to make it a conductor, it is necessary to have oxygen vacancies so that tungsten oxide with some oxygen missing will activate the electrode. Moreover argon is an inert gas, so it does not react with the tungsten oxide structure but will help to remove the oxygen atoms that have been released.

4.4.1 WO_3 deposition on stainless steel strip electrode via Approach III:

Electrodeposition:

Stirring the electrolyte during WO_3 deposition using a fresh $W_2O_{11}^{-2}$ solution and purging the solution with Ar is the best combination to improve the electrodeposition

results. Approach III gave a smooth electrodeposition, as shown in Figure 57. The plot below shows the best results achieved up to that point.

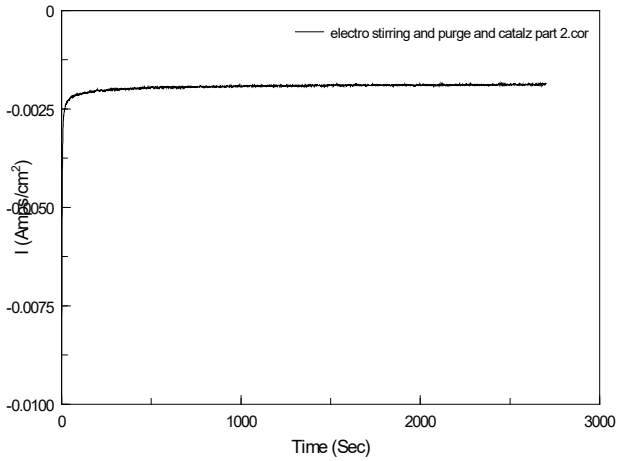

Figure 57. WO_3 electrodeposition on a stainless steel strip electrode via Approach III.

Once the electrodeposition is done, the strip has taken on a dark blue color, as shown in Figure 58 below.

Figure 58. Electrodeposited WO_3 film on stainless steel strip via Approach III.

After the electrodeposition, the stainless steel electrode was washed with ethanol and DI water, and then allowed to air dry. After that, it was heated to 450°C with argon.

The picture in Figure 59 below shows how it looked after the thermal treatment; its color had become yellow, consistent with nanoparticulate WO_3.

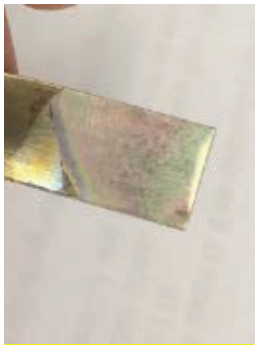

Figure 59. WO_3 film on stainless steel strip electrode prepared via Approach III and after thermal treatment at 450°C under Ar.

SEM and EDX results for Approach III WO_3 coating:

The thickness of the tungsten oxide film was about 1 μm before annealing. After annealing it is about 0.7 μm.

The steel strip electrodes are cut from a larger sheet. The sheet is processed at the manufacturer in such a way that one side has a rougher finish than the other. One side has nearly a mirror finish, while the other is decidedly less smooth. The smooth side will be designated the front face, while the rougher one will be the back face. It was found that the characteristics of a WO_3 film would vary, depending on which side was exposed facing the other electrodes in the deposition cell. The following micrographs were taken on the front face:

Front face (high magnification):

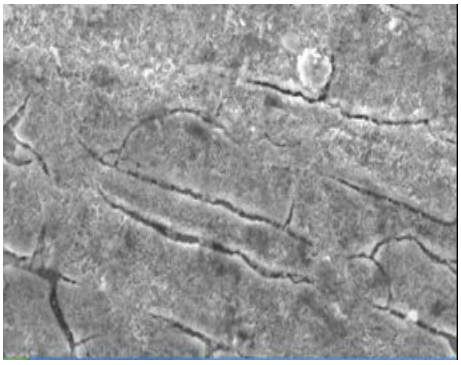

Element	Wt%	At%
CK	04.67	16.77
OK	15.85	42.68
NaK	02.35	04.41
ClK	01.34	01.63
CrK	06.16	05.10
MnK	00.99	00.78
FeK	20.81	16.05
NiK	02.77	02.03
WL	45.06	10.56
Matrix	Correction	ZAF

Figure 60. High magnification SEM-EDX data for tungsten oxide electrodeposition via Approach III on steel strip annealed with Ar at 450°C; front face.

Front face (low magnification):

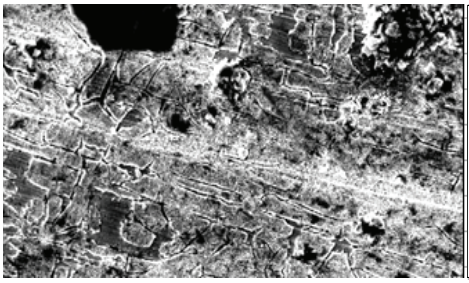

Element	Wt%	At%
CK	06.30	20.92
OK	16.68	41.58
NaK	03.12	05.41
ClK	01.45	01.63
CrK	06.12	04.69
MnK	00.87	00.63
FeK	19.47	13.91
NiK	02.72	01.85
WL	43.29	09.39
Matrix	Correction	ZAF

Figure 61. Low magnification SEM-EDX data for tungsten oxide electrodeposition via Approach III on steel strip electrode and annealed under Ar at 450°C; front face.

The images of the front face are very close to those seen earlier. In those micrographs the structures are more connected. However, the film does not look uniform; it is disorganized because water evaporation during the annealing created a rough surface. Moreover, after annealing there are many areas without film coverage. Electron microscopy data for stainless steel strip before electrodeposition is shown in Figure 62 below.

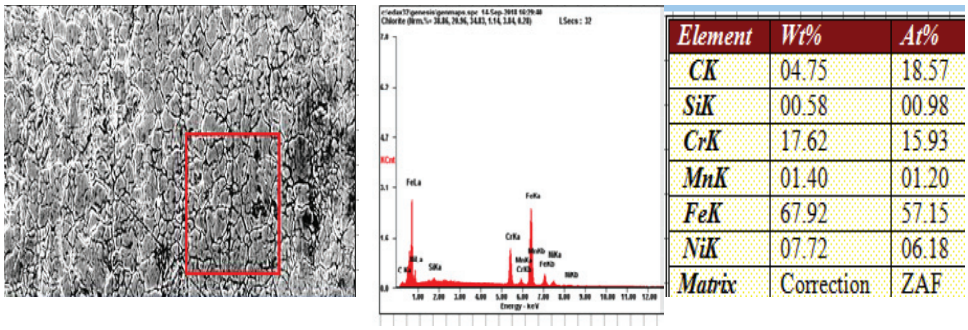

Element	Wt%	At%
CK	04.75	18.57
SiK	00.58	00.98
CrK	17.62	15.93
MnK	01.40	01.20
FeK	67.92	57.15
NiK	07.72	06.18
Matrix	Correction	ZAF

Figure 62. SEM-EDX data for the front face of a stainless steel strip before electrodeposition but after cleaning.

The surface of the substrate looks amorphous. There are many small closely spaced structures which are randomly dispersed. The elemental analysis is what was expected: high concentrations of iron, carbon and chromium. The EDX results are very similar to the commercial stainless steel composition, which has a minimum of 18% chromium and 8% nickel.

Figure 63 and Figure 64 are from the back face:

Back face (high magnification):

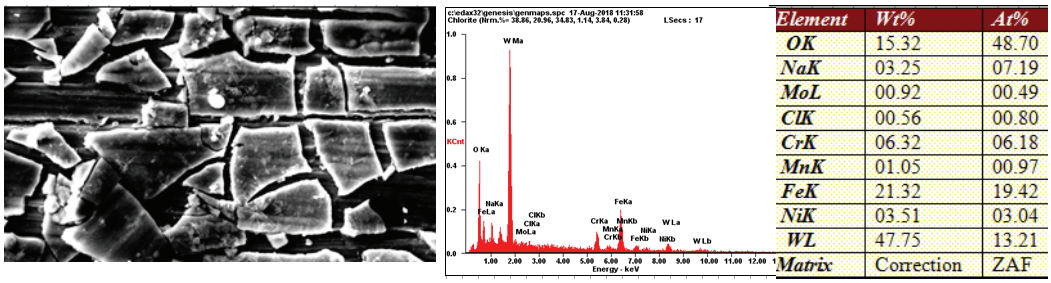

Element	Wt%	At%
OK	15.32	48.70
NaK	03.25	07.19
MoL	00.92	00.49
ClK	00.56	00.80
CrK	06.32	06.18
MnK	01.05	00.97
FeK	21.32	19.42
NiK	03.51	03.04
WL	47.75	13.21
Matrix	Correction	ZAF

Figure 63. SEM-EDX data for tungsten oxide electrodeposition on a steel strip after annealing at 450°C under Ar; back face

Back (low magnification):

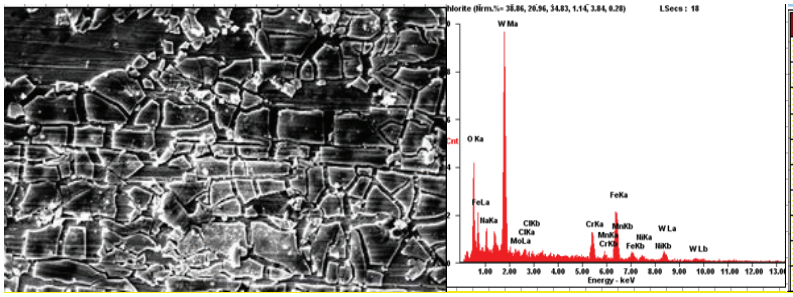

Element	Wt%	At%
OK	14.36	45.44
NaK	03.38	07.45
MoL	01.23	00.65
ClK	00.96	01.37
CrK	07.33	07.14
MnK	00.95	00.87
FeK	23.96	21.71
NiK	03.76	03.24
WL	44.07	12.13
Matrix	Correction	ZAF

Figure 64. SEM-EDX data for tungsten oxide electrodeposition on a steel strip after annealing at 450°C under Ar; back face

Figure 63 and Figure 64 look disorganized too, with areas having no film coverage. This surface is smoother than films on the front surface.

In the backside pictures, the structures are less connected than in the front. But the connection is better than if the samples had not been heated with argon.

Microscopy data for the back face of a strip are given in Figure 65.

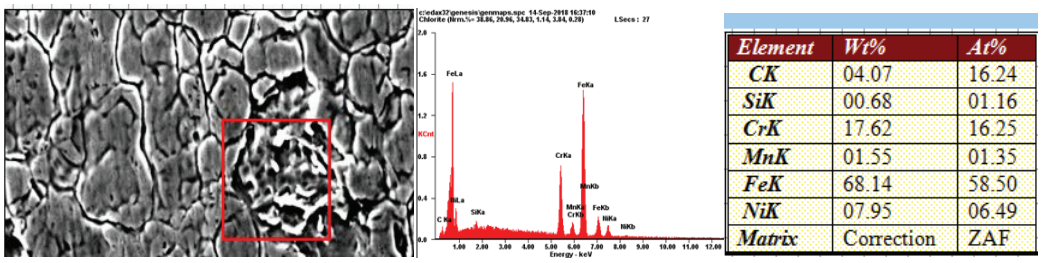

Element	Wt%	At%
CK	04.07	16.24
SiK	00.68	01.16
CrK	17.62	16.25
MnK	01.55	01.35
FeK	68.14	58.50
NiK	07.95	06.49
Matrix	Correction	ZAF

Figure 65. SEM-EDX data for the back face of a stainless steel strip.

The surface of the substrate looks amorphous as well. There are narrow cracks around the structures, but there is no pattern. The elemental analysis is what was

expected, and it was very similar with the substrate for the front face analysis described above.

Table 5 summarizes the elemental analysis of the WO_3 films after argon annealing.

Table 5. EDX Elemental Analysis for stainless steel film

	Front (high magnification)		***Front (low magnification)***		***Back (high magnification)***		***Back (low magnification)***	
	(Weight %)	***At %***	***(Weight %)***	***At %***	***(Weight %)***	***At %***	***(Weight %)***	***At %***
O	15.85	42.65	16.68	41.58	15.32	48.70	14.36	45.44
W	45.06	10.56	43.29	9.39	47.75	13.21	44.07	12.13

The EDX results show uniform concentration of tungsten and oxygen on the different samples. The front face had O deficit, while the back face had O surplus. The atomic percentage results do not agree well with the stoichiometric values, but they are closer than Approaches I and II.

Photoelectrochemistry results: WO_3 on steel strip electrode

The Figure 66 shows the photoelectrochemistry behavior of the strip after annealing under argon:

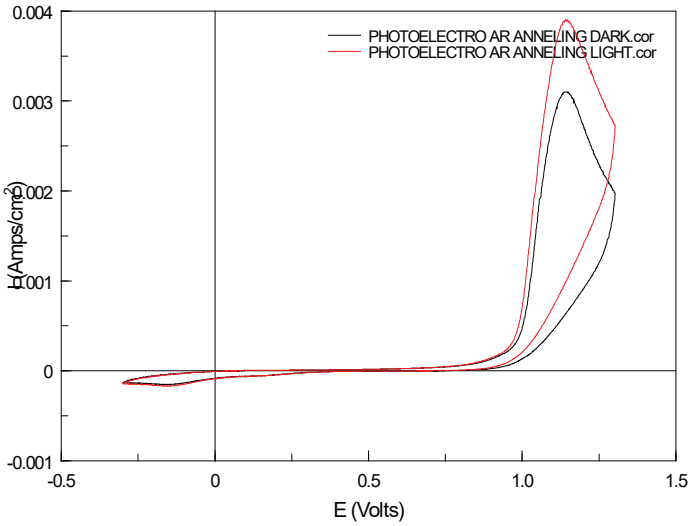

Figure 66. Photoelectrochemistry of WO_3 on stainless steel strip in 0.1 M H_2SO_4.

There was no photovoltage between light and dark. After the photoelectrochemistry experiment, which was run with an electrolytic solution of 0.1 M H_2SO_4, the electrode was observed under the electron microscope again to check if the film was still there. The results were not positive. The SEM-EDX analysis of the electrode after photoelectrochemistry is shown in Figure 67 and Figure 68.

Front face deposition:

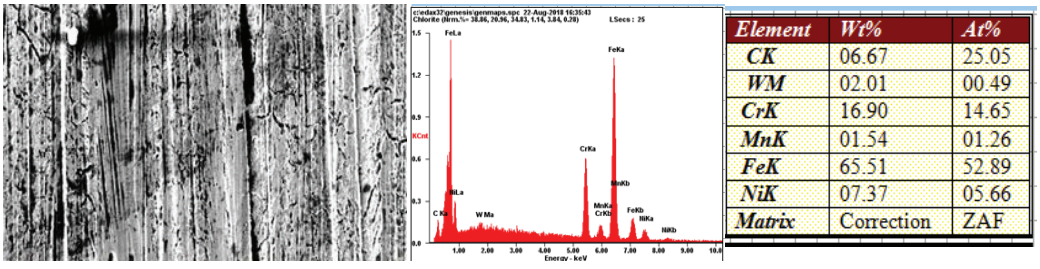

Element	Wt%	At%
CK	06.67	25.05
WM	02.01	00.49
CrK	16.90	14.65
MnK	01.54	01.26
FeK	65.51	52.89
NiK	07.37	05.66
Matrix	Correction	ZAF

Figure 67. SEM-EDX data for WO_3 on stainless steel strip electrode after the photo electrochemistry experiments; front face, (magnification: 1100x)

Back face deposition:

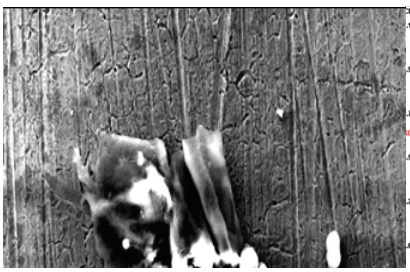

Element	Wt%	At%
CK	24.99	60.81
WM	01.29	00.21
CrK	13.60	07.65
MnK	01.62	00.86
FeK	52.52	27.49
NiK	05.98	02.98
Matrix	Correction	ZAF

Figure 68. SEM-EDX data for WO_3 on stainless steel strip electrode after the photo electrochemistry experiments; back face.

The micrographs in Figure 67 and Figure 68 show there was no tungsten oxide film on the stainless steel. Previous research suggests that peroxide can attack the tungsten oxide film when there are high positive voltages. It makes sense because the peroxide was used to make the film. Peroxide has the effect of lowering the photocurrent over periods of time and slowly damaging the film by re-dissolving the tungsten oxide. Water can be partially oxidized to peroxide, which then reacts with the tungsten oxide (17).

$$2H_2O \rightarrow 2H^+ + H_2O_2 + 2e^- \qquad E^0 = 1.77V \text{ vs NHE} \quad (17)$$

In this experiment, 1.3 V was the maximum potential imposed, so that peroxide may have formed via another mechanism, such as partial reduction of O_2 that was generated via electrolysis.

As a possible alternative method for observing a photovoltage, the addition of potassium hexacyanoferrate (II) (5 mM) to sulfuric acid (0.1 M) electrolyte was attempted. It will help to see better the photovoltaic effect without high positive voltage.

The results are shown in Figure 69 below.

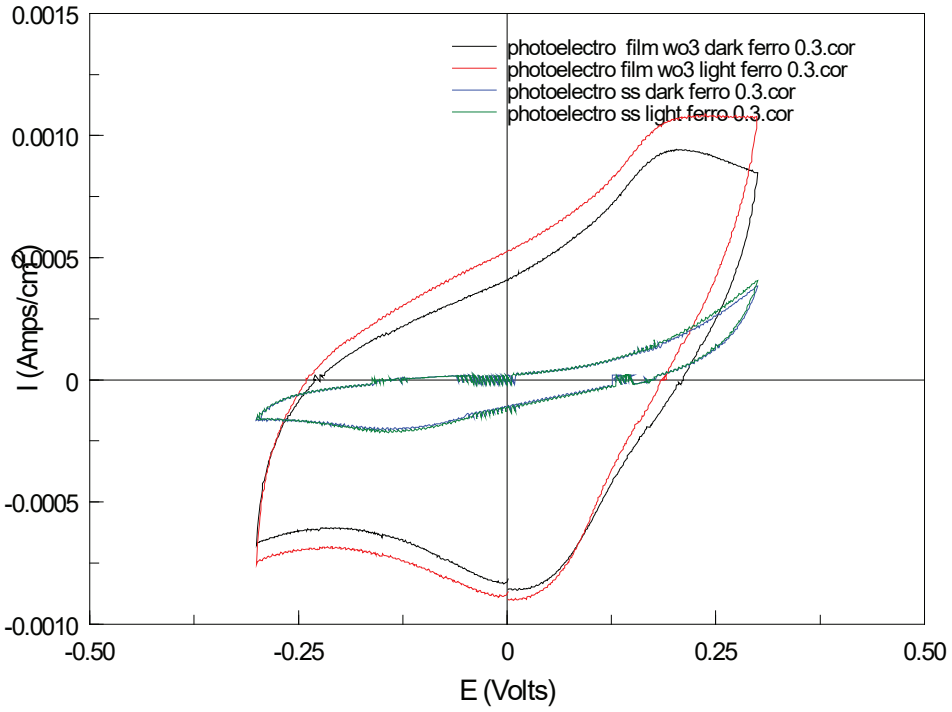

Figure 69. Effect of $K_4[Fe(CN)_6]$ on the photoelectrochemistry of WO_3-on steel strip electrode (Approach III). Conditions: 0.1 M H_2SO_4 and potassium hexacyanoferrate(II) (5 mM), sweep rate 50 mV/s from -0.3 to +0.3 V vs silver chloride; dark and under illumination.

There are four curves in the graph. The blue curve is the behavior of the stainless steel electrode in the dark. The green curve is the photoelectrochemical behavior of the stainless steel electrode in the light. The black curve is in the dark. The red curve is the photoelectrochemical behavior of the tungsten oxide on stainless 304 electrode in the light. The plot gives a good indication that the tungsten oxide electrode is highly active in the potassium hexacyanoferrate (II) solution. It was also observed that the stainless steel electrode is largely inactive in this electrolyte. Within this voltage range the

tungsten oxide strip did not suffer any damage. The only disappointing result was that the red curve should have shifted to more negative potentials. In addition, if the light was manually chopped (blocked) during the cyclic voltammetry, there was no immediate response in the curve, implying no photo activity. Nevertheless, just getting some activity for the oxidation of the ferro to ferric and ferric back to ferro, reasonable behavior, though not strictly reversible, is an improvement. The fact that hexacyanoferrate (II) is active on tungsten oxide but not on stainless steel is proof that the tungsten oxide film is there, and can be used as an active electrode.

For reversible curves, the peak to peak separation, for one electron transfer, is 60 mV. In the plot above, it is about 180 mV. It means that the kinetics are slower than ideal, but it shows clearly the oxidation. The fact that there are substantial currents with the tungsten oxide coating surface as compared with the planar stainless steel, indicates the tungsten oxide is an active surface, through which the charge could be transferred. It is not inert.

X ray diffraction:

An X-ray diffraction spectrum for WO_3 on stainless 304 is shown in Figure 70.

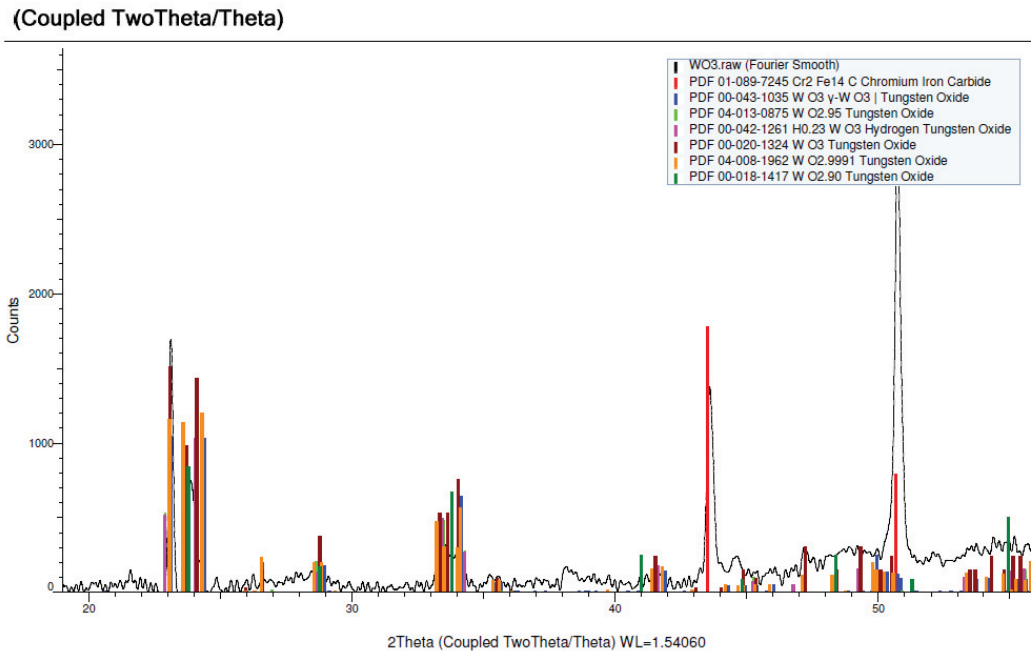

Figure 70. X-ray diffraction spectrum of WO_3 on stainless 304 (Approach III).

The X-ray results show that the sample is a mixture of different tungsten oxide phases. It contains hydrogen tungsten oxide $H_{0.23}WO_3$ (monoclinic). It was expected to have a monoclinic phase because it is the most stable at room temperature. The two large peaks at the end of the spectrum are related to the stainless steel substrate. The sample was annealed under argon flow at 450 °C.

4.4.2 Photoelectrochemistry of WO_3 on Steel Thread (Approach III)

The photoelectrochemical tests were run for the WO_3-coated thread, annealed at 450 °under Ar (Approach III).

The results are shown in Figure 71:

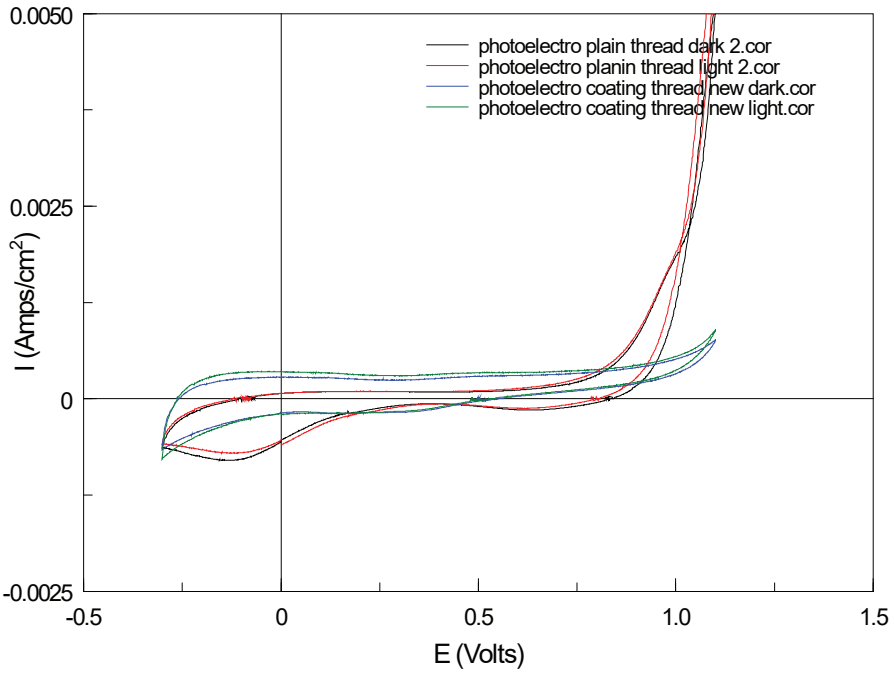

Figure 71. Light/dark voltammetry of steel thread and WO_3-coated threads in 0.1 M H_2SO_4. Annealed at 450°C with argon flow.

The red and black curve corresponds to the naked thread behavior. The red one is under illumination and the black is in the dark. Figure 71 shows there is a lot of iron oxidation due to the sharp current rise at the (+) vertex potential, and some reduction indicated by the small negative peak in the negative potential region. As a consequence of the high level of oxidation, the Fe^{+3} signal must originate from the steel thread electrode. The green and blue curves correspond to the tungsten oxide-coated thread. The blue curve is in the dark and the green curve under illumination. The green and blue spectra show reduced iron oxidation, but there is still not an appreciable photocurrent for

the purpose of this research. Figure 72 shows the photoelectrochemical behavior for different potential limits.

The test did not sweep far enough positive to see O_2 because the supporting electrolyte was at low pH The standard redox potential (pH = 0) for the water/O_2 redox couple is 1.23 V (vs NHE). At pH 1, it effectively lowers to 1.17 V. Evolution of O_2 cannot occur below that potential. In fact, O_2 evolution is such a slow reaction that considerably higher applied potentials are necessary to achieve significant gas evolution

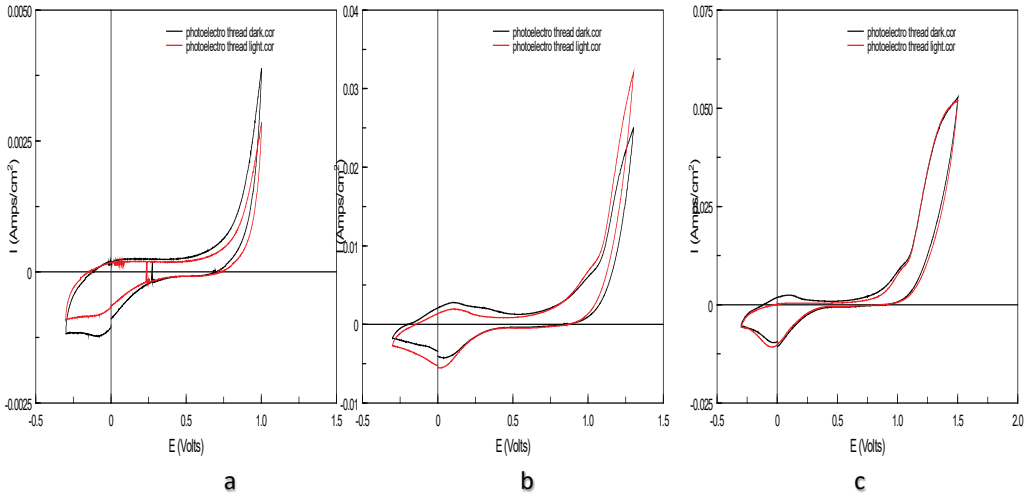

Figure 72. Light/dark voltammetry for steel thread and WO_3-coated thread in 0.1 M H_2SO_4, in three different voltage ranges (coated thread WE). Annealed at 450 °C with argon flow (Approach III).

The curves do not show significant photo potentials between light and dark. When the positive potential increases above 1.3 V, there is no unexpected reduction peak as had occurred with the stainless steel substrate. However, if very high positive potential is imposed, the WO_3 coating is lost, just as it happened with the stainless steel substrate. The voltammetric activity is interpreted as oxidation of the iron content in the

steel thread, some of which is dissolved into the sulfuric acid electrolyte. The negative potential sweep then shows a reduction of ferric ion to ferrous, which is then available for reoxidation with peak potential just positive of the AgCl reference zero. The results continue to be negative, because the red voltammogram should be shifted to more negative potentials. The photoactivity is still blocked.

In order to find the best annealing conditions, there were other experiments where the post-deposition annealing was performed at 600 °C. The results are shown in

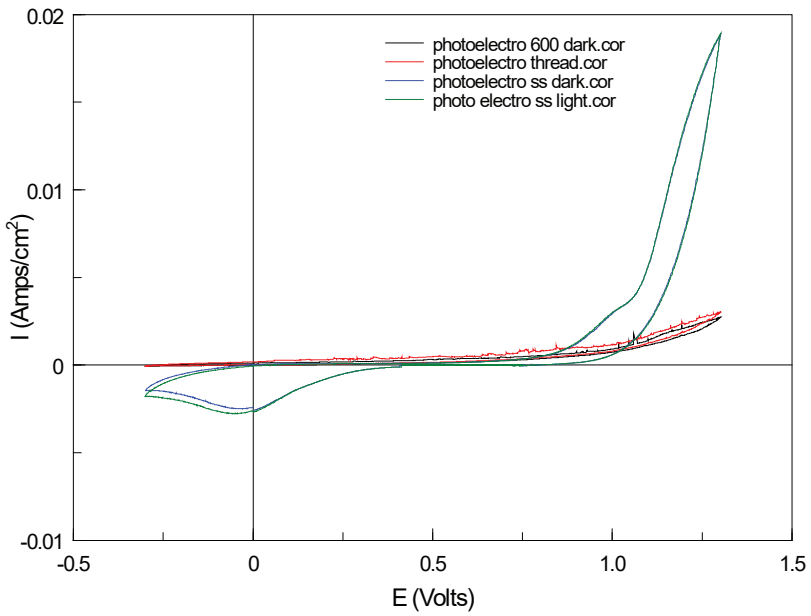

Figure 73:

Figure 73. Light/dark voltammetry of steel thread and WO_3-coated threadfin 0.1 M H_2SO_4. Annealed at 600 °C under argon flow (Approach III).

The blue and green curves correspond to the naked thread behavior. The green curve is under illumination and the blue curve is in the dark. Figure 73 shows there is a

lot of iron oxidation, and some iron reduction. The black and red curves correspond to the WO_3-coated thread. The black curve was taken in the dark and the red curve was taken under illumination. Comparing the plot at 600 °C to the plot at 450 °C, the first one is four times the other scale, 20 mA vs 5 mA. On the other hand, both WO_3-coated voltammograms are very quiet and flat. The fact that the voltammograms are flat and quiet is a good sign, because it would indicate that the WO_3 coating is reasonably conductive and electrochemically stable between the vertex potentials. It may also mean that the WO_3 electrode is inactive toward any redox species, however, and so it may be necessary to try other methods, like a platinum coating, to activate the surface of the electrode.

So far, the plot at 450 °C and the plot at 600 °C are showing that the coating is protecting the steel wire from oxidation, so it is a corrosion inhibitor.

Figure 74 shows the photoelectrochemical behavior of WO_3-coated steel thread for different potential limits.

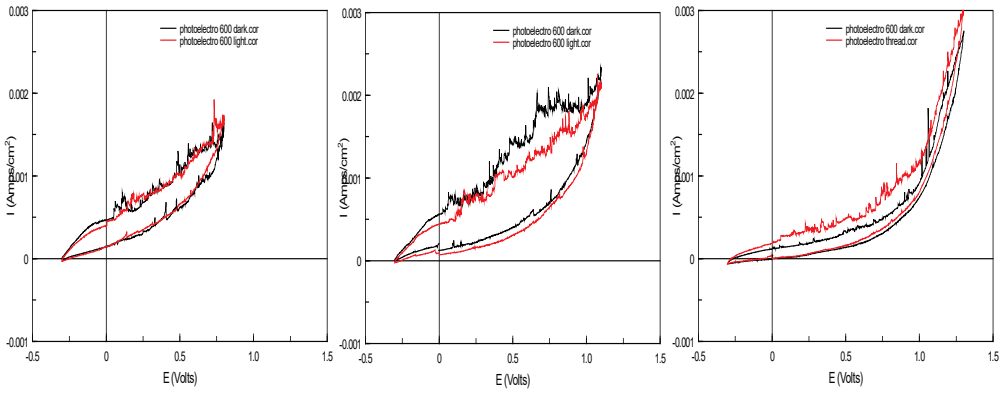

a b c

Figure 74. Light/dark voltammetry of steel thread and WO_3-coated thread in 0.1 M H_2SO_4, for three different voltage ranges. Annealed at 600 °C under argon flow.

The curves on Figure 74 do not show significant photo potentials between light and dark. The three plots show noise. The noise could be associated with the rehydrating process, which changes the surface area. The curves look more noisy on the anodic sweep and less noisy on the cathodic sweep. Those facts could imply that something is unstable. In addition, in voltammogram C, the dark spectrum has higher currents than the illuminated curve. If the photovoltaic effect was present, the red spectra should exhibit a photocurrent and the onset of faradaic processes should be shifted to more negative potential. The photoactivity is still minimal. In fact, 450 °C gave results with less instability, so the next experiments should anneal at 450 °C (18). Previous research has reported that 450 °C is the optimum annealing temperature with the highest photoactivity. Annealing temperatures beyond 450 °C caused deterioration in the photoactivity of the WO_3 film. (5) (19).

It was suspected that the Pyrex 3-neck round bottom flask that contained the electrolyte was absorbing most of the light (borosilicate glass is known to have a UV cut-off wavelength of about 340 nm, so we already knew that the strongest photons were not reaching the electrode), and for this reason the photoelectrochemical effect could not be observed. Due to the previous circumstances, the 3-neck round bottom flask was replaced with a test tube that contained a quartz flat window through which light could go without being absorbed or deflected.. The photoelectrochemical results are shown in Figure 75:

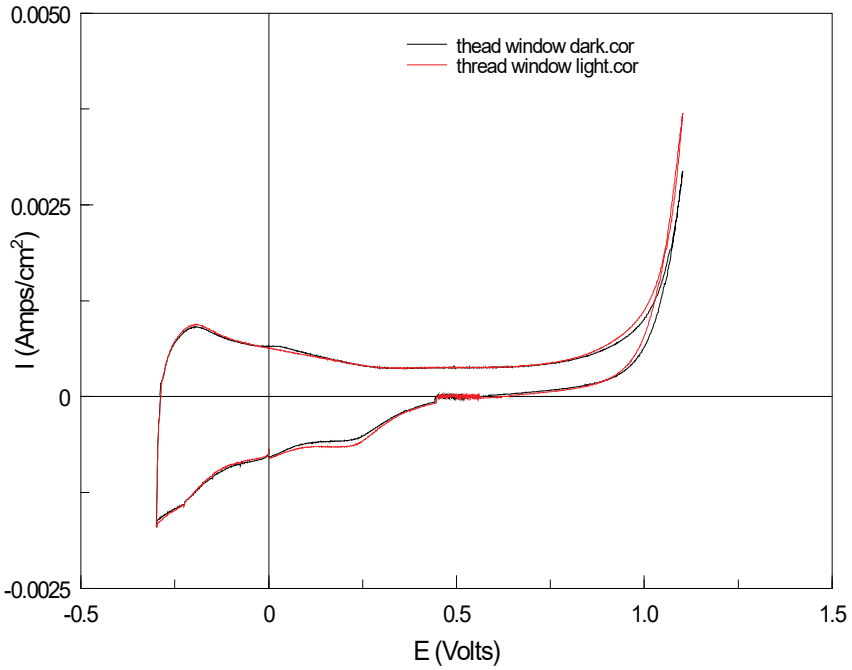

Figure 75. Light/dark voltammetry of WO_3 on steel thread in 0.1 M H_2SO_4 and illuminated through a quartz window. Annealed at 450 °C under argon flow (Approach III).

The Figure 75 illustrates that electrode shows fair activity for hydrogen, both reduction and oxidation. There is no photovoltage.

The next step should be to add a platinum coating on the top of the tungsten oxide strip in order to have a continuous coating. It will help to activate the electrode and to have a photovoltaic current.

4.5 Approach IV Results:

The behavior that has been observed so far is that tungsten oxide forms an ohmic contact with the steel, which has a work function of around 4.5 eV. A higher work

function metal, like platinum, which is 5.1 eV, should improve the band bending. The base strategy for getting band bending and developing a depletion layer in the junction between two phases is to develop the sloping electric field effect that is necessary to have a high work function metal with a n-type semiconductor, such as tungsten oxide to get a photovoltaic effect.

If an oxygen atom is missing from the WO_3 lattice, then two of the W atoms surrounding that vacancy must be reduced (from W^{6+} to $W^{5+)}$ due to overall charge neutrality of the material. The outermost electron in W^{5+} is rather energetic, however, and is easily thermally promoted into the conduction band. That is the basis of a vacancy-doped, n-type material.

4.5.1 Thread Electrodeposition:

The potentiostatic current-time curve for the electrodeposition of WO_3 on steel thread via Approach IV is shown in Figure 76:

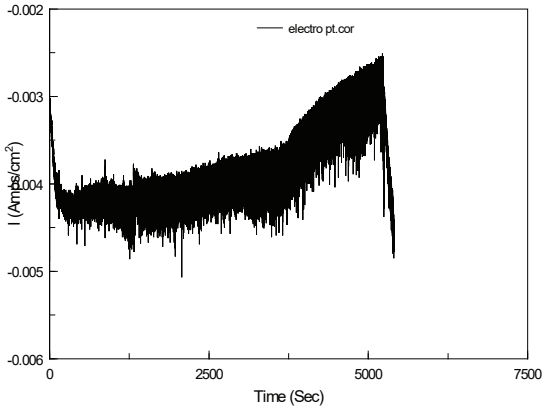

Figure 76. Potentiostatic current-time curve for the electrodeposition of WO_3 on steel thread under Approach IV.

The curve was noisy. It could be associated with the stirring and movement of the thread in the electrolyte. When three minutes were left to finish, the chloroplatinic acid hexahydrate was added. An immediate result from the addition at 5000 s was a cathodic current increase in the plot. In theory, the platinum coating has a thickness around 0.2 µm,

4.5.2 Photoelectrochemistry Thread Electrode:

The photoelectrochemistry tests were run for the WO_3-coated thread, annealed at 450 °C with Approach IV. The result is shown in Figure 77:

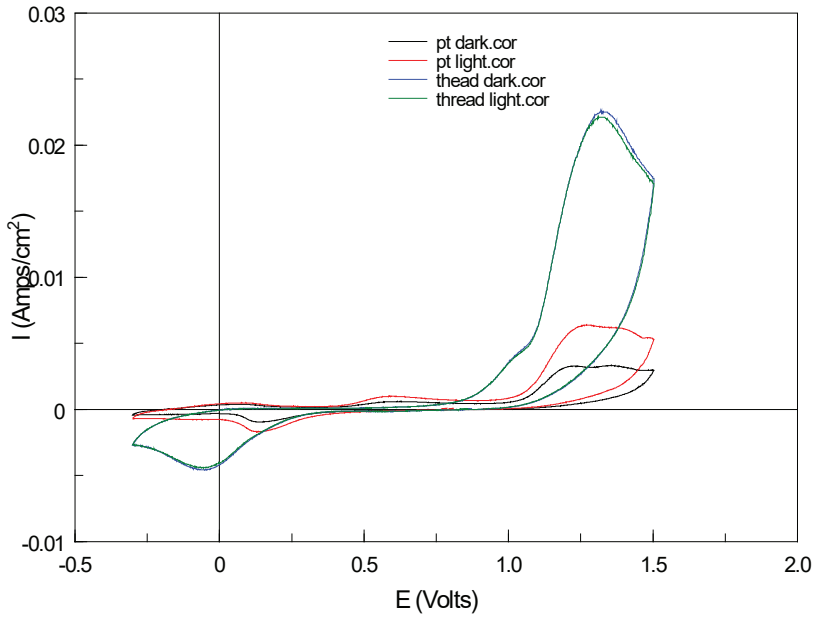

Figure 77. Light/dark voltammetry of Pt-WO_3 on steel thread (Approach IV) in 0.1 M H_2SO_4. Annealed at 450 °C under argon flow.

The green and blue curves correspond to the naked thread behavior. The green curve is under illumination and the blue curve is in the dark. The black and red curves correspond to the coated tungsten oxide thread. The black curve is in the dark and the red curve is under illumination. Both WO_3- voltammograms are very quiet and flat, which is a desired behavior. The WO_3-coated thread is working as a corrosion inhibitor for the steel substrate as well. There is a small photovoltage between the light and the dark. If the photovoltage is calculated close to the onset of oxygen (1.1 V), it is around 0.06V (comparing the red and black curves).

The voltammetric curves below in Figure 78 show the photoelectrochemical behavior for different potential ranges.

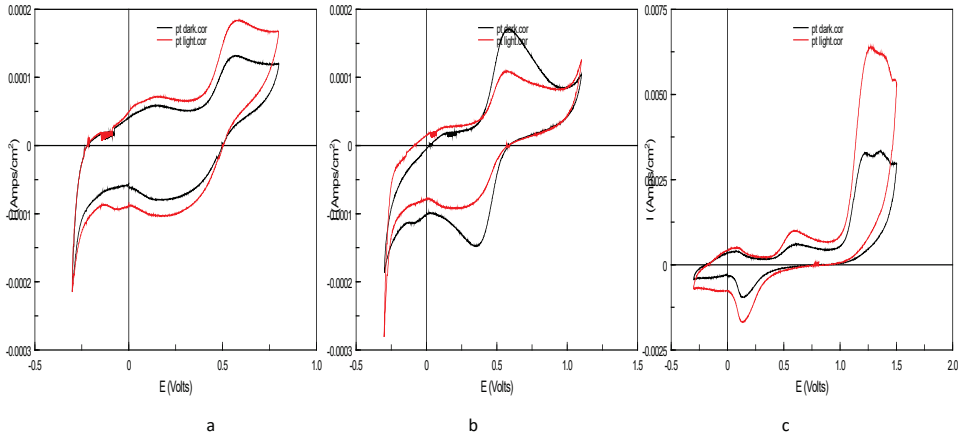

Figure 78. Light/dark voltammetry of Pt-WO_3-coated steel thread in 0.1 M H_2SO_4, in three different voltage ranges Annealed at 450 °C under argon flow (Approach IV).

Curves a and c show a photo potential between the light and the dark. If the photo voltage in the curve c is calculated close to the onset of oxygen (1.1 V), is around 0.1 V (comparing the red and black curves).

In addition, in plot b; the dark voltammogram actually has higher currents than the illuminated curve. In all three curves, the current at the (-) vertex potential rises more sharply than before; it indicates that the platinum coating is facilitating hydrogen evolution. The peaks in the middle are correlated because they have similar sizes and are associated with platinum oxidation and reduction. There is no significant photo effect yet, but it is a small improvement, nevertheless.

4.5.3 SEM - EDX:

The micrographs were taken once the photoelectrochemistry experiment was done.

The results are shown in Figure 79:

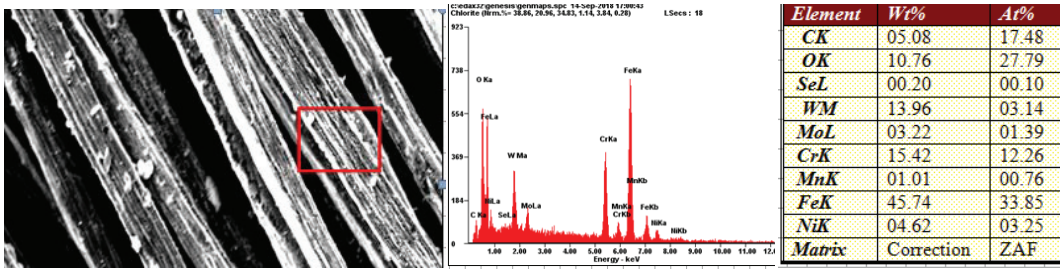

Element	Wt%	At%
CK	05.08	17.48
OK	10.76	27.79
SeL	00.20	00.10
WM	13.96	03.14
MoL	03.22	01.39
CrK	15.42	12.26
MnK	01.01	00.76
FeK	45.74	33.85
NiK	04.62	03.25
Matrix	Correction	ZAF

Figure 79. SEM – EDX of Pt – WO_3 coating on steel thread after the photo electrochemistry experiment.

WO_3 coverage of the steel thread was minimal. The tungsten concentration is lower than previous values. Moreover, there is no platinum concentration. This fact

could be associated with dissolution of the coatings due to peroxide or iron dissolution when high positive voltages are applied (17).

4.6 Approach V Results:

The indium tin oxide coated glass is applied widely as an electrode. Approach V repeated the procedure described before, but instead of a conductive thread, it uses ITO as a working electrode.

4.6.1 WO_3 Electrodeposition on ITO:

Potentiostatic WO_3 electrodeposition on ITO gave the current-time curve shown in Figure 80:

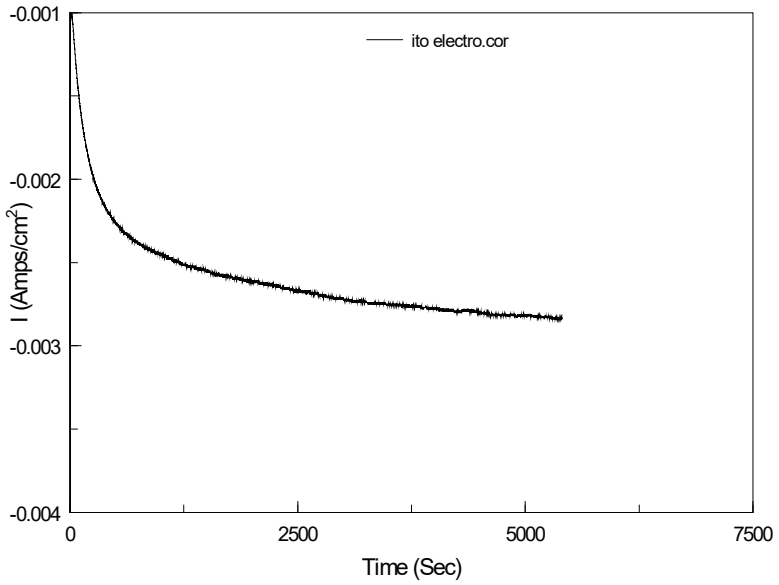

Figure 80. WO_3 electro deposition on ITO (Approach V)

The curve was smooth, and process was very quiet and successful. At the end, the ITO has a continuous blue film on top, as shown in Figure 81:

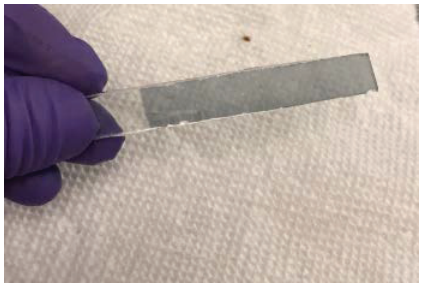

Figure 81. ITO substrate after tungsten oxide electrodeposition.

The coating film was annealed at 450 °C under air. Once it was finished, the coating was still there but its color had turned yellow. Figure 82 shows the oxidized film:

Figure 82. ITO substrate after air annealing at 450 °C

The film in Figure 82 is fragile due to its porous nature and could be wiped off easily

4.6.2 SEM - EDX of ITO Electrode:

The ITO electrode was observed under the SEM, and it gave the following image, as shown in Figure 83:

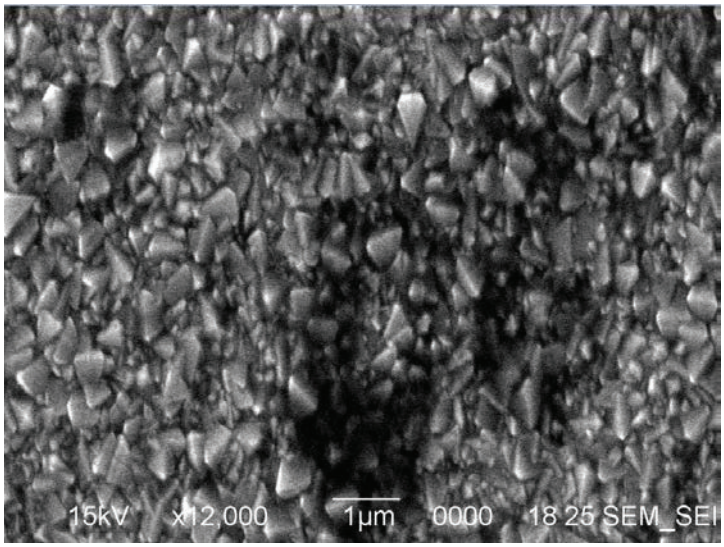

Figure 83. ITO surface without WO_3 coating, (magnification: 12000x)

Figure 83 shows there are no cracks around the particles, unlike the WO_3 film. Instead, there are connected particles. EDX results are shown in Figure 84:

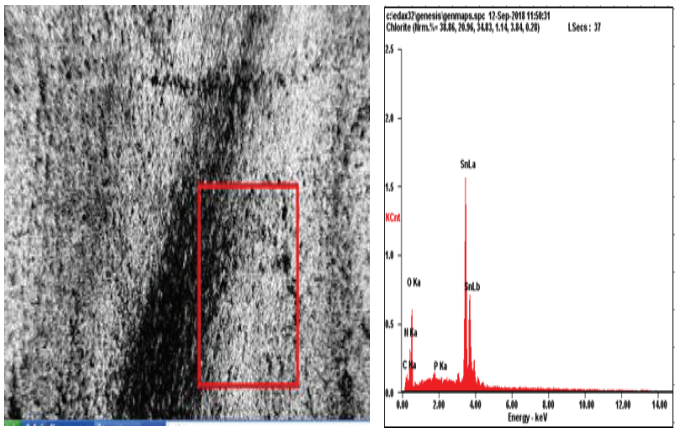

Element	Wt%	At%
CK	03.07	08.96
NK	07.03	17.61
OK	24.60	53.94
PK	00.22	00.24
SnL	65.08	19.24
Matrix	Correction	ZAF

Figure 84. EDX analysis of ITO surface.

The EDX results are close to what was expected: high concentration of tin (Sn) and oxygen. Micrographs of a tungsten oxide coating on ITO is shown in Figure 85:

Figure 85. SEM of WO_3 coating on ITO substrate, (magnification: 900x, 3300x, 10000x left to right)

Figure 85 shows a smooth surface; it was smoother than the WO_3 film on stainless steel. It was observed that the cracks' widths are narrower than on stainless steel. There was another difference found; there are small particles on the cracks of the WO_3- ITO electrode. In general terms, the WO_3 film is more uniform on the ITO substrate. The EDX gave the following results (Figure 86):

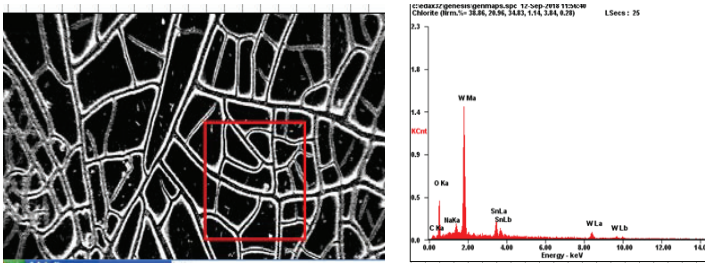

Element	Wt%	At%
CK	01.67	07.26
OK	20.31	66.40
NaK	00.79	01.80
SnL	16.50	07.27
WL	60.72	17.27
Matrix	Correction	ZAF

Figure 86. EDX results for WO_3 coating on ITO, (magnification: 900x)

The EDX results are close to what was expected: high concentration of tungsten (W), tin (Sn) and oxygen. The indium concentration was very low, so the EDX technique could not recognize this low concentration.

4.6.3 Photoelectrochemistry ITO Electrode:

Figure 86 shows the photoelectrochemical behavior for different voltage ranges.

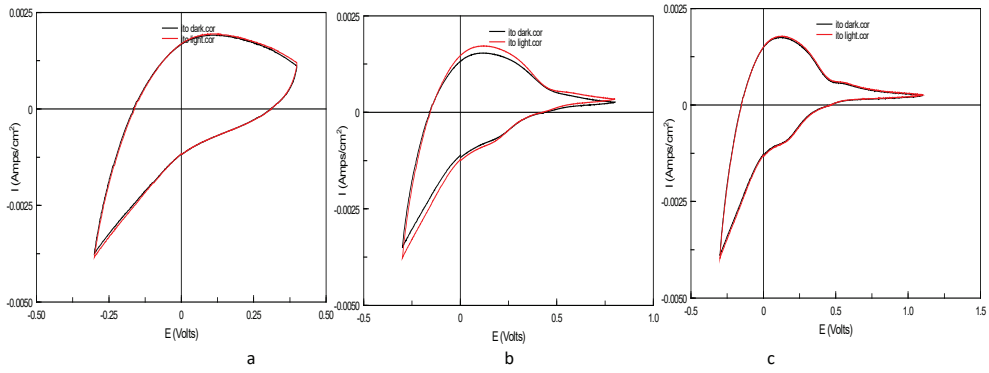

Figure 87. Light/dark voltammetry of WO_3 on ITO in 0.1 M H_2SO_4, in three different voltage ranges; annealed at 450 °C under argon flow (Approach V)

The curves in Figure 87 do not show any photo potential between light and dark.

Conclusion

Tungsten oxide electrodeposition on steel thread was achieved. However, the photovoltaic clothing application requires a different synthesis or it needs continued work on the platinum coating experiments, which gave positive results, but can be improved. The WO_3 films prepared by electrodeposition and precursor preparation had a small degree of nanocrystallinity. The size of the WO_3 grain is dominated by the precursor tungsten concentration and deposition time (5). The photovoltaic clothing application requires a method that offers a high degree of nano-crystallinity. The synthesis of WO_3 nanocrystals will improve its photoactivity because the large surface-to-volume ratio increases the effective surface area for charge transfer across interfaces In addition, the transport mechanisms, electronic band structure and optical properties in nano-crystalline semiconductors, under illumination, are different from the bulk material due to its small size. However, the optimum WO_3 crystal size has to be a compromise between optimum surface area and the rate of surface charge recombination (5). It was found that the morphology of the WO_3 nano film is strongly affected by the precursor solution as well. So, the idea to continue developing the electrodeposition and precursor preparation procedure is worth evaluating.

The annealing procedure for the thread and the stainless steel 304 strips was not successful in air, because the tungsten oxide film did not attach well to the surface of the electrode. So, the electrode was heated under argon and turned blue-yellow. The blue color means it was highly doped and the space charge layer is very thin. This reason explains in part why it was not a good photovoltaic material.

The color change of the WO_3 film, from blue to yellow when the voltage was swept from negative to positive and vice-versa, suggests the material could be used for electrochromic applications. These properties make WO_3 a good candidate for manufacture of smart windows (20). For photovoltaics, it seems that when it is converted to yellow, it should be kept there. For the ITO case, the doping sites in the blue tungsten oxide are permanent unless they are heated to 450 ^oC in air, so the lattice opens up some sites and forces the oxygen to fill those vacancies. Vacancies formed are stable at room temperature.

The electrodeposition on the ITO surface gave one of the best results, as the WO_3 film was very uniform and organized in each case. It had a smooth surface. The steel substrate had an alignment problem because the WO_3 lattice spacings do not match with it.

The platinum coating gave an interesting result. The platinum helps with hydrogen evolution and it could help with the photocurrents as well. This phenomenon can be seen on the cyclic voltammetry curves by the pronounced and deep peak in the hydrogen reduction current.

Comparing the morphology of the WO_3 coating on the steel thread and the stainless steel 304 strips, they appear very similar. The coating has pretty sharp peaks and its surface is rough. It has many cracks around the amorphous shapes that are observed under the microscope. The thickness of the film is around 1.0 μm after the electrodeposition and around 0.7 μm after annealing with argon. In both cases, the thread

and the stainless steel substrates, the photo-activity is poor and it will be necessary to improve it.

References

1. **U.S. Energy Information Administration (eia).** [Online] January 2017. [Cited: April 24, 2019.] https://www.eia.gov/outlooks/steo/archives/jan17.pdf.

2. **Patha, Venu Gopal.** *Characterization of TiO2 Photoelectodes fabricated via Low Temperature Sintering Process.* Youngstown : Youngstown State University, 2011.

3. *Renewable Energy Course (Lecture 2).* **Linkous, Dr. Clovis.** Youngstown, OH : s.n., 2017. CHEM 6991.

4. *Photoelectrochemical properties and photocatalytic activity of nitrogen - doped nanoporous WO3 photoelectrodes under visible light.* **Yuyang, Liu, et al.** Xiangtan (China) : s.n.

5. *Nanostructured Tungsten Trioxide Thin Films Synthesized for Photoelectrocatalytic Water Oxidation: A review.* **Meng Nan Chong, Zhu and Chan, Eng Seng.** s.l. : Wiley Online Library. 2974-2997.

6. **Rhoden, Linkous and Mettee.** *Development of a hydrogen evolving photocatalytic membrane.* Youngstown, OH : s.n., 2012.

7. *Nanoestructured tunsten oxide - properties, synthesis, and applications.* **Zheng, Haidong, et al.** s.l. : Materials Views, 2011. 10.1002/admf.201002477.

8. **www.wikipedia.com.** ***Photovoltaic Effect.*** **[Online] November 20, 2017.**

9. www.wikipedia.com. ***Tungstene Trioxide.*** **[Online] November 20, 2017.**

10. Rutto, Patrick. ***Electrodeposition of CdTe on Stainless Steel 304 Substrate.*** **Youngstown State University : s.n., 2018. pp. 9,10.**

11. Hull, R, et al., [ed.]. ***Spring Series in Material Science.*** **p. 423.**

12. Ed. D.R. Lide, CRC Press, [ed.]. ***Handbook of Chemistry and Physics.*** **Eighty-first.**

13. https://www.adafruit.com/product/640. [Online] [Cited: January 10, 2019.]

14. Kalapala, Sreevani. ***Removal of Hydrogen Sulfide from Landfill Gas Using a Solar Regenerable Adsorbent*** **. Youngstown : Youngstown State University, 2014.**

15. pmpaspeakingofprecision.com. ***Hardness vs.Hardenability - There is a difference.*** **[Online] PMPA, 07 09, 2009. [Cited: March 15, 2018.]**

16. Skoog, Douglas A., Holler, F. James and Crounch, Stanley R. ***Principle of Intrumental Analysis.*** **Belmont : CENGAGE Learning, 2007.**

17. ***Effect of Electrolytes on the Selectivity and Stability of n-type WO3 Photoelectrodes for Use in Solar Water Oxidation.*** **Hill, James C and Choi, Kyoung-Shi. Lafayette : ACS Publications, 2012. 7612-7620.**

18. ***Anneling induced microstructural evolution of electrodeposited electrochromic tungsten oxide films.*** **Deepa, M., et al. New Delhi : s.n., 2005.**

19. ***Effect of Annealing Temperature on Photoelectrochemical Properties of WO3/Fe2O3 Photoelectrodes.*** **Ng, K.H., et al. Kuching, Malaysia : s.n., 2014. 3rd IET International Conference on Clean Energy And Technology (CEAT) 2014.**

20. ***Facile fabrication of WO3 crystalline nanoplate on FTO glass and their application in electrochromism.*** **Chu, Jia, et al. 11, 2016, Vol. 11, pp. 749-752. 1750-0443.**

21. ***Study of Electrodeposited Tungsten Trioxide Thin Films.*** **Kang, Pei, t and Tsung, Alfred. UK : s.n., 1992. 1141-1147.**

22. ***Electrodeposition of nano-granular tungsten oxide thin films for smart window application.*** **More, A.J, et al. India : Elsevier, 2014. 298-301.**

23. Cotton, F. Albert and Goefrey Wilkinson. ***Advance Inorganic Chemistry.*** **s.l. : Interscience Publishers.**

24. ***Effect of Electrolytes on the Selectivity and Stability of n-type WO3 Photoelectrodes for Use in Solar Water Oxidation.*** **James C., Hill and Kyoung-Shin, Choi. West Lafayette : s.n.**

25. ***Size Effectt of WO3 nanocrystals for photooxidation of water in particulate suspension and photoelectrochemical film systems.*** **Hong, Suk Joon, et al. Pohang (South Korea) : s.n.**